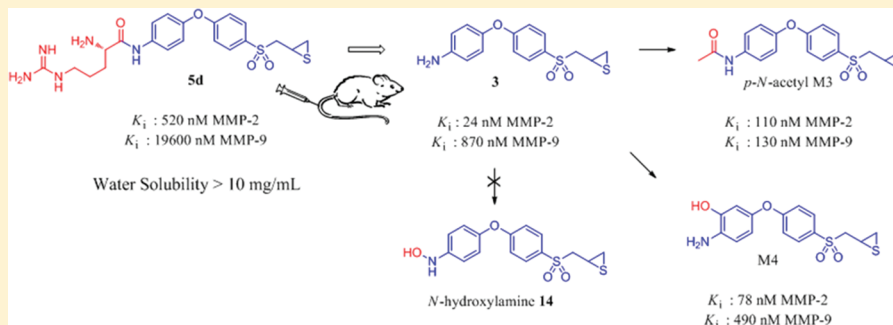# Selective Water-Soluble Gelatinase Inhibitor Prodrugs

Major Gooyit,[†,§] Mijoon Lee,[†,§] Valerie A. Schroeder,[‡] Masahiro Ikejiri,[†] Mark A. Suckow,[‡] Shahriar Mobashery,[†] and Mayland Chang*,[†]

[†]Department of Chemistry and Biochemistry and [‡]Freimann Life Sciences Center and Department of Biological Sciences, University of Notre Dame, Notre Dame, Indiana 46556, United States

ABSTRACT:

SB-3CT (**1**), a selective and potent thiirane-based gelatinase inhibitor, is effective in animal models of cancer metastasis and stroke; however, it is limited by poor aqueous solubility and extensive metabolism. We addressed these issues by blocking the primary site of metabolism and capitalizing on a prodrug strategy to achieve >5000-fold increased solubility. The amide prodrugs were quantitatively hydrolyzed in human blood to a potent gelatinase inhibitor, ND-322 (**3**). The arginyl amide prodrug (ND-478, **5d**) was metabolically stable in mouse, rat, and human liver microsomes. Both **5d** and **3** were nonmutagenic in the Ames II mutagenicity assay. The prodrug **5d** showed moderate clearance of 0.0582 L/min/kg, remained mostly in the extracellular fluid compartment (Vd = 0.0978 L/kg), and had a terminal half-life of >4 h. The prodrug **5d** had superior pharmacokinetic properties than those of **3**, making the thiirane class of selective gelatinase inhibitors suitable for intravenous administration in the treatment of acute gelatinase-dependent diseases.

■ INTRODUCTION

Matrix metalloproteinases 2 and 9 (MMP-2 and MMP-9) are zinc-dependent endopeptidases that are also known as gelatinases. The unregulated activities of these enzymes have been implicated in a host of human diseases, including tumor invasion and metastasis, cardiovascular and neurological diseases, and inflammation to name a few.[1−4] Gelatinases were shown to be essential for leukocyte penetration into the brain parenchyma in a mouse model of experimental autoimmune encephalomyelitis.[5] All of these diseases involve restructuring of the extracellular matrix for manifestation of the disease;[4,6−8] hence, selective gelatinase inhibitors are highly sought.[9,10]

We have described the first highly selective mechanism-based gelatinase inhibitor, (4-phenoxyphenylsulfonyl)methylthiirane (SB-3CT, **1**).[11] This inhibitor undergoes a chemical transformation within the active site of gelatinases, a process that is likely at the root of the selectivity that the compound exhibits in its potent inhibition.[12] Compound **1** is efficacious in animal models of prostate cancer metastasis to the bone,[13] breast cancer metastasis to the lungs,[14] and T-cell lymphoma metastasis to the liver.[15] Compound **1** also blocks the MMP-9-dependent degradation of the extracellular matrix protein laminin and thus rescues neurons from apoptotic cell death in a mouse model of transient focal cerebral ischemia.[16] In addition, **1** prevents laminin degradation

and neuronal death in a rat model of subarachnoid hemorrhage,[17] a type of hemorrhagic stroke. Compound **1** significantly reduces flow-induced vascular remodeling, an adaptive process that allows blood vessels to normalize hemodynamic stress in response to increased blood flow in atherosclerosis, aneurysms, and brain arteriovenous maltransformations in mice.[18] In a rat model of spinal cord injury, treatment with **1** results in decreases in MMP-9 activity, extravasation, and apoptotic cell death.[19] This novel inhibitor has found use in many other biological systems, which we will not outline here in the interest of brevity.

SB-3CT, 1

X = OH, **2**
X = NH₂, **ND-322 (3)**
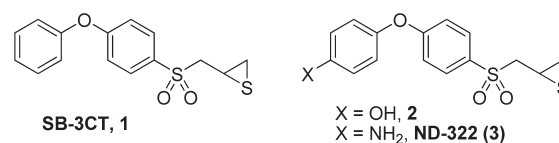
Despite documented excellent biological activity, administration of **1** to animals is problematic due to its poor water solubility of 2.3 μg/mL.[20] Because of poor solubility, the compound is typically dosed as a suspension intraperitoneally. Furthermore, it

Table 1. Structures of Ester and Amide Prodrugs


X		
Gly	**4a**	**5a**
L-Lys	**4b**	**5b**
L-Glu	**4c**	**5c**
L-Arg	**4d**	**ND-478 (5d)**
L-Arg- L-Arg	**4e**	**5e**

is rapidly metabolized by hydroxylation at the *para*-position of the terminal phenyl ring (**2**) to a more potent gelatinase inhibitor than the parent **1** and by oxidation at the α-position to the sulfonyl that leads to the formation of the inactive sulfinic acid.[21] We addressed oxidation at the α-position to the sulfonyl by the addition of a methyl substituent at that site; however, this modification led to a 10-fold decrease in inhibitory potency.[22] However, derivatization at the *para*-position of the terminal phenyl ring with methanesulfonate did not only improve metabolic stability but also enhanced potency.[23]

Our interest in developing therapeutics for the treatment of acute neurological conditions such as stroke, aneurysm, and traumatic brain injury, for which intravenous infusion is the preferred route of administration, led us to explore increasing the water solubility of **1**. For parenteral administration, a solubility of 10 mg/mL is usually needed to adequately formulate a drug.[24] This presented a delivery challenge in the case of **1**, which was administered intraperitoneally as a suspension in studies of animal models of disease. A prodrug strategy is useful to solve formulation problems associated with poor aqueous solubility. A prodrug (drug + promoiety) is a chemical entity with little or no pharmacological activity, which undergoes transformation (biological or otherwise) to a therapeutically active drug.[25] The majority of prodrugs for parenteral administration have modifications where a polar ionizable promoiety is introduced to increase water solubility.[25] Amino acid promoieties have been employed to improve the aqueous solubility of drugs containing an alcohol or amine[26,27] and are rapidly and quantitatively converted to the active drug by the action of esterases and/or peptidases in blood. We surmise that functionalization at the *para*-position of the terminal phenyl ring with water-solubilizing agents to create prodrugs might address the solubility problem of **1**, as well as block the primary site of metabolism. We used amino acids (and a peptide) as promoieties to impart water solubility to the gelatinase inhibitor. The *p*-hydroxy derivative **2** is a good candidate for ester conjugation, as it was previously shown to be a more potent gelatinase inhibitor than **1**.[21] We also explored the use of the *p*-amino derivative **3**, which was found to have potent gelatinase inhibitory activity, to synthesize aminoacid—amide conjugates. The resulting ester and amide prodrug series (Table 1) are expected to undergo hydrolysis in plasma and blood to release the active gelatinase inhibitors **2** or **3**. The syntheses and evaluation of the properties of these prodrug series, compounds **4** and **5**, are the subjects of this article.

Scheme 1. Synthesis of 3[a]
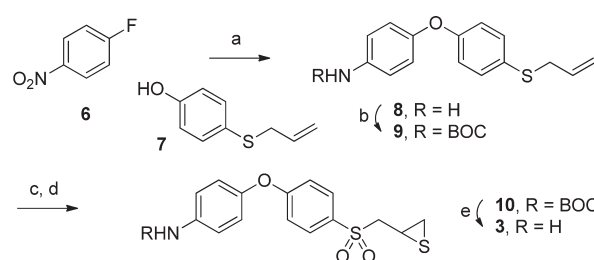
[a] Reagents and conditions: (a) (i) Cs_2CO_3, room temperature, 2 h; (ii) Zn, AcOH, 0 °C to room temperature, 2 h, 79%. (b) Boc_2O, Et_3N, MeOH, 60 °C, 2 h, 82%. (c) *m*-CPBA, CH_2Cl_2, room temperature, 72 h, 81%. (d) Thiourea, MeOH/CH_2Cl_2, room temperature, 18 h, 72%. (e) 4 N HCl in 1,4-dioxane, ethyl acetate/CH_2Cl_2, 0 °C to room temperature, 48 h, 82%.

■ RESULTS AND DISCUSSION

Syntheses of Prodrugs. The *p*-aminophenoxybenzene scaffold in **3** was assembled by the methodology developed by Ikejiri et al.,[28] which is the coupling of 1-fluoro-4-nitrobenzene (**6**) and 4-(allylthio)phenol (**7**) under basic conditions, followed by reduction of the nitro group to the amine over elemental zinc in acetic acid (Scheme 1). The resulting amine **8** was treated with di-*tert*-butyl dicarbonate to give the Boc-protected compound **9**. The Boc group was chosen as the amine-protecting group because sulfonylmethylthiirane is relatively stable under the acidic condition that is used for the removal of Boc at the end of the synthesis (see transformation of **10** to **3**). The rest of the transformations, including the oxidation to sulfone, epoxide formation using *m*-chloroperoxybenzoic acid (*m*-CPBA), and thiirane conversion using thiourea, were performed by the methodology developed by us earlier.[29,30] Removal of the Boc group in compound **10** was carried out in the presence of 4 N HCl in 1,4-dioxane at room temperature for 48 h to yield **3** as the HCl salt in 82% yield.

The syntheses of amino acid conjugates of phenol **2** and of aniline **3** as prodrugs of gelatinase inhibitors are outlined in Scheme 2. Compound **2**, prepared according to the literature,[23] was acylated with Boc-protected *N*-hydroxysuccinimide (NHS) esters of amino acids (Gly, L-Lys, L-Glu, and L-Arg) or a peptide (L-Arg-L-Arg) in the presence of 4-(dimethylamino)pyridine (DMAP) to give the esters **11**. The Boc group in compounds

Scheme 2. Syntheses of the Ester and Amide Prodrugs[a]
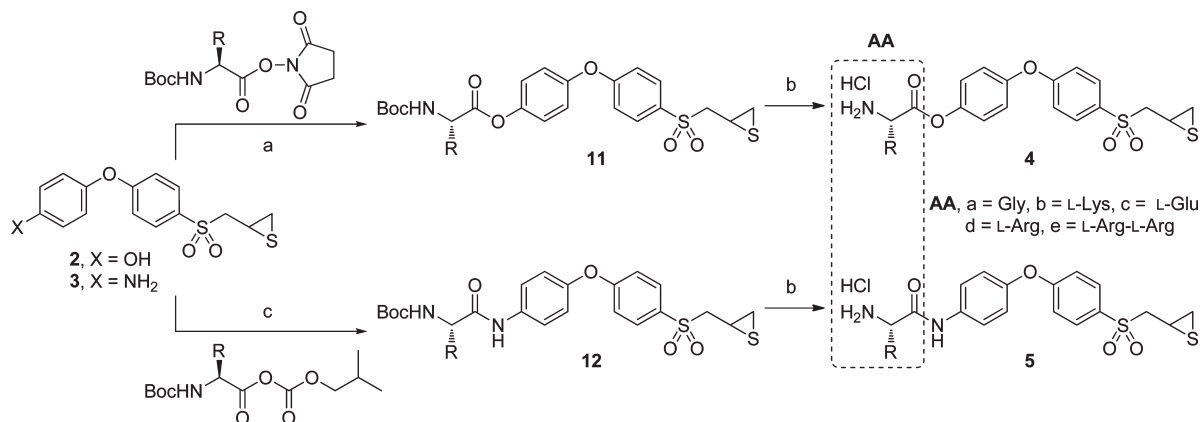
[a] Reagents and conditions: (a) DMAP, iPr$_2$EtN, CH$_2$Cl$_2$, room temperature, 3 h, 72−81%. (b) 4 N HCl in 1,4-dioxane, ethyl acetate/CH$_2$Cl$_2$, 0 °C to room temperature, 48 h, 71−79%. (c) THF, −20 °C to room temperature, 1 h, 61−79%.

Table 2. Ex Vivo Hydrolyses of Amide Prodrugs of 3

amide prodrugs	half-life at 37 °C (min)		aqueous solubility (mg/mL)
	human plasma	human blood	
5a	32.4 ± 2.7	27.1 ± 2.5	>10[a]
5b	25.1 ± 5.2	15.3 ± 1.9	>10[a]
5c	32.8 ± 3.6	27.9 ± 3.8	>10[a]
5d	29.5 ± 0.7	25.4 ± 0.1	>10[a]
5e	11.8 ± 0.5	5.9 ± 0.6	>10[a]

[a] Because of the limited sample supply, no further effort was made to measure the maximum solubility.

11, in turn, was readily removed by treatment with 4 N HCl in 1,4-dioxane to result in the ester prodrugs 4. The acid treatment for the removal of the Boc group in the presence of thiirane worked well, as described in Scheme 1 for the synthesis of 3.

When 3 was subjected to the same acylation conditions (using NHS esters of an amino acid), the desired amide bond was not formed. Instead, it gave only the recovery of the two starting materials. The Boc-protected amino acid was activated to a mixed anhydride by the treatment of isobutyl chloroformate in the presence of N-methylmorpholine and was allowed to react with 3 to give the desired amide linkage. The removal of the Boc group in compounds 12 was carried out by acid treatment resulting in the amide prodrugs 5.

Aqueous Solubility and ex Vivo Hydrolyses of Prodrugs. The aqueous solubilities of the prodrugs were assessed by UV spectroscopy (see Experimental Section). The solubility of compounds 4 and 5 exceeded 10,000 μg/mL, which indicates a significant enhancement in aqueous solubility over that of the parent 1 (2.3 μg/mL) of over 5000-fold. Next, we explored the stability of compounds 4 and 5 in aqueous solution. The ester prodrugs 4 were unstable under aqueous conditions, and within 2 h, the aqueous solutions turned turbid. The precipitate was analyzed and was confirmed as compound 2. The instability of the ester prodrugs in aqueous solution might be due to the promotion of a water molecule by the aminoacyl moiety itself for hydrolysis of the ester group or by intermolecular aminolysis of the ester moiety by the free amino group(s) in the promoiety.
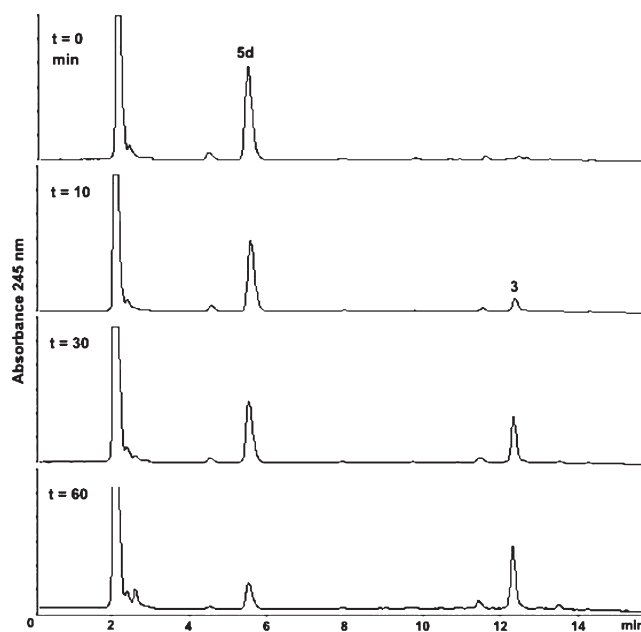

Figure 1. Ex vivo hydrolysis of 5d in human blood generates 3.

Hence, the ester derivatives 4 would appear to be inherently unstable under these conditions. However, the corresponding amide derivatives 5 were stable in aqueous solution for over one month, as assessed by HPLC.

We subsequently explored the properties of the prodrugs in the presence of human plasma and human whole blood. The ester prodrugs 4 hydrolyzed completely in human plasma within 2 min. In contrast, the amide derivatives 5 displayed increased stability in human plasma. The half-lives of the amide prodrugs in human plasma and whole blood are summarized in Table 2. The amide prodrugs 5a−d quantitatively released the active constituent 3 in human plasma within 30 min. Whereas the half-life for hydrolysis of the dipeptide variant 5e was shorter in the series, the hydrolytic enzymes in plasma first gave rise to the mono-arginine variant 5d, which experienced further hydrolysis to 3. Hydrolyses of the amide conjugates were in general more rapid in whole blood than in plasma, significantly so in the case of

Table 3. Kinetic Parameters for the Inhibition of Gelatinases

	MMP-2			MMP-9[a]		
amide prodrugs	$10^{-3} k_{on}$ (M^{-1}s^{-1})	$10^4 k_{off}$ (s^{-1})	K_i (μM)	$10^{-3} k_{on}$ (M^{-1}s^{-1})	$10^4 k_{off}$ (s^{-1})	K_i (μM)
5a	1.9 ± 0.6	8.2 ± 0.9	0.44 ± 0.05	0.21 ± 0.04	6.5 ± 0.6	3.1 ± 0.3
5b	3.4 ± 0.1	2.1 ± 0.9	0.062 ± 0.025	0.27 ± 0.04	4.2 ± 0.7	1.6 ± 0.3
5c	2.5 ± 0.1	1.8 ± 1.6	0.069 ± 0.064	0.28 ± 0.02	12.0 ± 0.7	4.3 ± 0.4
5d	1.5 ± 0.1	7.6 ± 2.9	0.52 ± 0.20	0.031 ± 0.006	6.0 ± 0.3	19.6 ± 1.0
5e	1.5 ± 0.1	6.1 ± 2.1	0.42 ± 0.15	0.044 ± 0.004	8.3 ± 2.3	18.7 ± 5.6
3	8.9 ± 0.2	2.1 ± 1.3	0.024 ± 0.015	0.61 ± 0.01	5.3 ± 0.7	0.87 ± 0.11

[a] Catalytic domain.

Table 4. Half-Life and Apparent Intrinsic Clearance in Liver Microsomes

	5d		3	
	half-life	$CL_{int,app}$	half-life	$CL_{int,app}$
species	(min)	(mL/min/kg)	(min)	(mL/min/kg)
mouse	>60	<47	27.3 ± 2.1	102.8 ± 7.9
rat	59.3 ± 4.5	23.7 ± 1.8	23.4 ± 0.7	60.0 ± 1.8
human	>60	<10	>60	<10

compounds 5b and 5e. The time-dependent release of 3 from the arginyl amide prodrug 5d is depicted in Figure 1.

Gelatinase Inhibition. The kinetics of gelatinase inhibition of the amide prodrugs is given in Table 3. The amide prodrugs showed slow-binding behavior in the inhibition of gelatinases, but the activities were consistently worse for the prodrugs, compared to that of the active constituent 3, which is released from them. Several general observations can be made of these compounds. First, the rate constants for the onset of inhibition (k_{on}) are rapid, and the rate constants for the reversal of inhibition (k_{off}) are slow. From the ratio of k_{off}/k_{on}, the dissociation constants (K_i) are evaluated. Compound 3, the species that is released from the prodrugs, is the most effective of the compounds listed in Table 3, inhibiting the enzymes with K_i values in the nanomolar range.

Metabolic Stability in Mouse, Rat, and Human Liver Microsomes. The in vitro metabolism of 5d and 3 was further evaluated in mouse, rat, and human liver microsomal incubations. The prodrug 5d was metabolically stable, as indicated by half-lives of 60 min or longer in mouse, rat, and human liver microsomes (Table 4). The prodrug 5d was more metabolically stable than 3. Compound 3 was stable in human liver microsomes, with $t_{1/2}$ > 60 min; the rates of metabolism in mouse and rat liver microsomes were faster, with $t_{1/2}$ values of 27.3 and 23.4 min, respectively. Compound 3 was significantly more metabolically stable than 1, which had a $t_{1/2}$ of 12.0 min in rat liver microsomes.[20]

Intrinsic clearance (CL_{int}), a measure of how readily the liver metabolizes a compound, was calculated from the in vitro half-lives. The prodrug 5d had intrinsic clearances of <47, 23.7, and <10 mL/min/kg in mouse, rat, and human, respectively, which were <50% of the hepatic blood flow (86, 66, and 21 mL/min/kg in mouse, rat, and human, respectively),[31] indicating that the compound would not be readily metabolized by the liver. Intrinsic clearances for 3 were 103, 60, and <10 mL/min/kg in mouse, rat, and human, respectively. Intrinsic clearances of 3
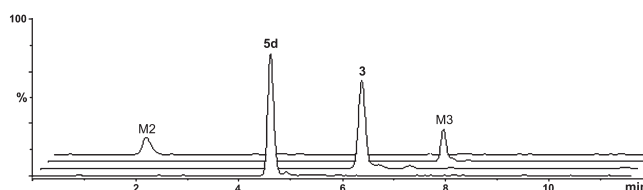

Figure 2. Reconstructed ion chromatogram following a 60-min incubation of 5d with rat S9 liver microsomes.

in the mouse and rat, in contrast to the case in human, were >70% hepatic blood flow, indicating that 3 was a higher-clearance compound in these species. In contrast, the prototype inhibitor 1 was readily metabolized and had an intrinsic clearance of 117 mL/min/kg in the rat, significantly higher than the hepatic blood flow of 66 mL/min/kg.[20] These data collectively indicate that 5d has superior pharmacokinetic properties compared to those of 3 and 1.

Metabolism Pathway. The metabolism of 5d was similar across species. The major metabolic pathway of 5d was hydrolysis to the active constituent 3 (Figure 2). Minor oxidation at the α position to the sulfonyl group to lead to the corresponding sulfinic acid M1 and N-acetylation of 3 to give M3 (Figure 2) were observed. M1 is not observed on the reconstructed ion chromatogram as it is a minor metabolite, and it readily experiences hydrolysis to give M2, which was detected. The prodrug 5d was hydrolyzed to 3 by amidases present in microsomes, and further oxidation gave its sulfinic acid metabolite M2. The identities of the sulfinic acids M1 and M2 were assigned on the basis of MS/MS spectra (Figure 3). We had previously observed a similar fragmentation pattern for the sulfinic acid of 1.[21] The identity of M3 was confirmed by comparison of the HPLC retention time and MS/MS spectrum (Figure 3) with those of an authentic synthetic standard, prepared as reported earlier.[28]
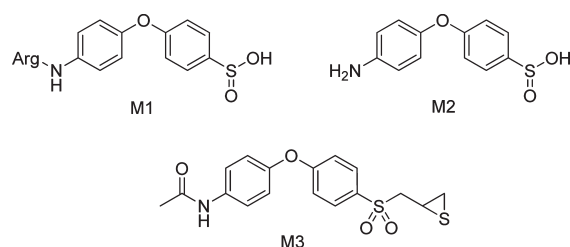
To gain further insight into the metabolism of 5d after the removal of the promoiety, we investigated the metabolism of 3. Incubation of 3 with liver microsomes showed oxidation at the α-position to the sulfonyl to give the sulfinic acid derivative M2.

To detect other minor metabolites of **3**, the ion chromatogram at m/z 338 $(MH + 16)^+$ was reconstructed (Figure 4, inset). The chromatogram displayed two peaks, labeled as M4 and M5, with distinct fragmentation patterns. Product ion mass spectrometric analysis of M5 showed cleavage of the sulfonyl-methylenethiirane linkage giving an ion at m/z 248, followed by a subsequent loss of sulfur to give a fragment at m/z 216, and further loss of two oxygens to generate the fragment at m/z 184. The product ion mass spectrum of **3** produced identical fragments at m/z 248, 216, and 184, indicating that the terminal phenyl ring and the middle phenyl ring were intact and that oxidation of the thiirane sulfur was the most likely transformation to account for the increase in mass of 16 amu in M5. Loss of 16 amu from MH^+ to
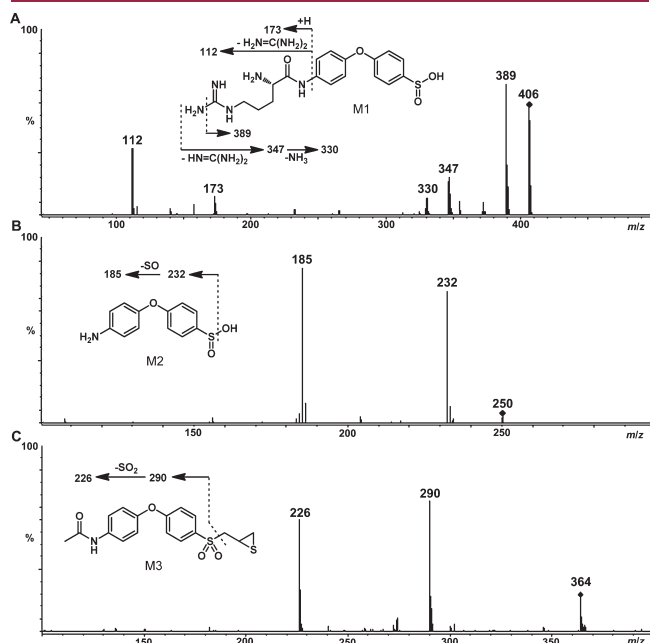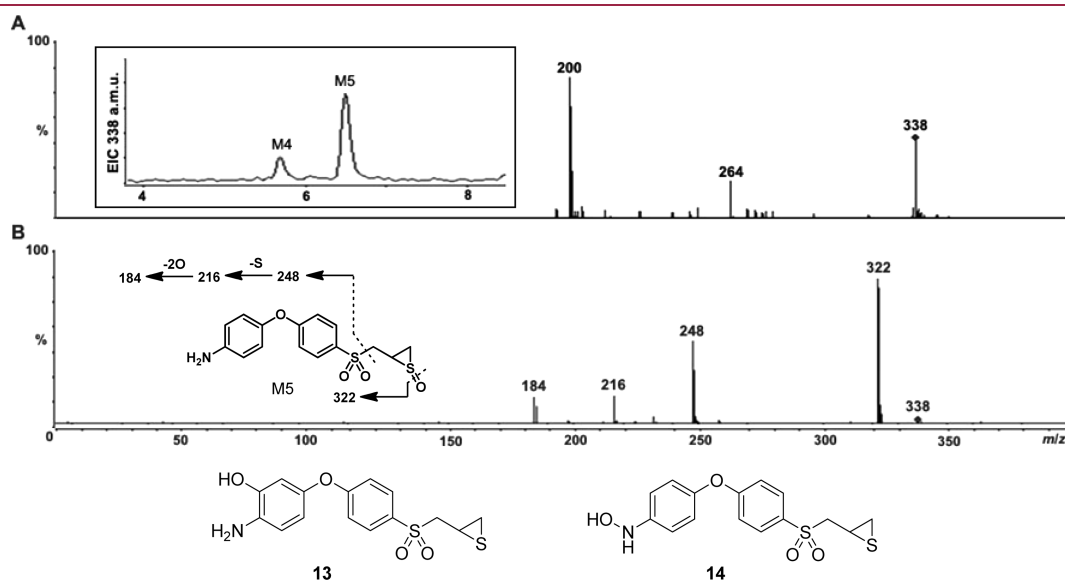

Figure 3. Product ion mass spectra of (A) metabolite M1 (MH^+, m/z 406), (B) M2 (MH^+, m/z 250), and (C) M3 (MH^+, m/z 364).

give a fragment at m/z 322 confirmed the assignment of M5 as the sulfoxide of **3**. We had seen this fragmentation previously for the sulfoxide metabolite of **1**.[21] The MS/MS spectrum of M4, however, indicated cleavage of the sulfonyl-methylenethiirane linkage to generate a fragment at m/z 264, 16 amu higher than that of **3**. Loss of SO_2 gave an ion at m/z 200. These data suggested the potential oxidation of the amino group or oxidation at the terminal phenyl or the middle phenyl ring. While hydroxylation of the middle ring is possible, we had not observed such an oxidative pathway for **1** and its derivatives previously.[21,22] Since the fragmentation pattern could not discriminate between the variant **13** and the *N*-hydroxylamine **14**, we prepared the authentic synthetic standards for each of compounds **13** and **14** to confirm the identity of the minor metabolite M4.

The synthesis of derivative **13** started by base-mediated coupling of the activated fluorobenzene **15** and phenolic **16** to yield **17**, followed by the reduction of the nitro group to the amine and subsequent *N*-Boc protection (Scheme 3). Basic hydrolysis of **18** at reflux selectively deprotected the thiophenol, which was then allowed to react with epichlorohydrin to generate the epoxide **19**. The succeeding steps involved oxidation to the sulfone **20**, conversion to the thiirane **21**, and final MOM and *N*-Boc removal by acid reflux to give **13**. A typical method to prepare *N*-hydroxylamine is the partial reduction of the nitro compound using zinc dust in the presence of ammonium chloride.[32] The transformation of the nitro derivative **22**, prepared as published,[28] to *N*-hydroxylamine **14** proceeded without decomposition of the thiirane moiety.

HPLC analysis revealed that M4 had an identical retention time as the synthetic **13** (Figure 5). Identification of M4 as derivative **13** was further confirmed by MS/MS analyses of M4 and the synthetic standards (Figure 6). Compound **13** had the identical product ion mass spectrum as metabolite M4. The MS/MS spectrum of the synthetic *N*-hydroxylamine **14** showed similar fragments (at m/z 264 and 200) as the metabolite. However, the ions at m/z 321, due to the loss of OH from the molecular ion, and at m/z 109, corresponding to the phenyl-hydroxylamine fragment, established that M4 was not the

Figure 4. Product ion mass spectra of (A) metabolite M4 and (B) M5, and (inset) a reconstructed ion chromatogram of m/z 338 $(MH + 16)^+$, following a 30-min incubation of **3** with rat liver microsomes.

Scheme 3. Syntheses of 13 and the N-Hydroxylamine 14 Derivative[a]
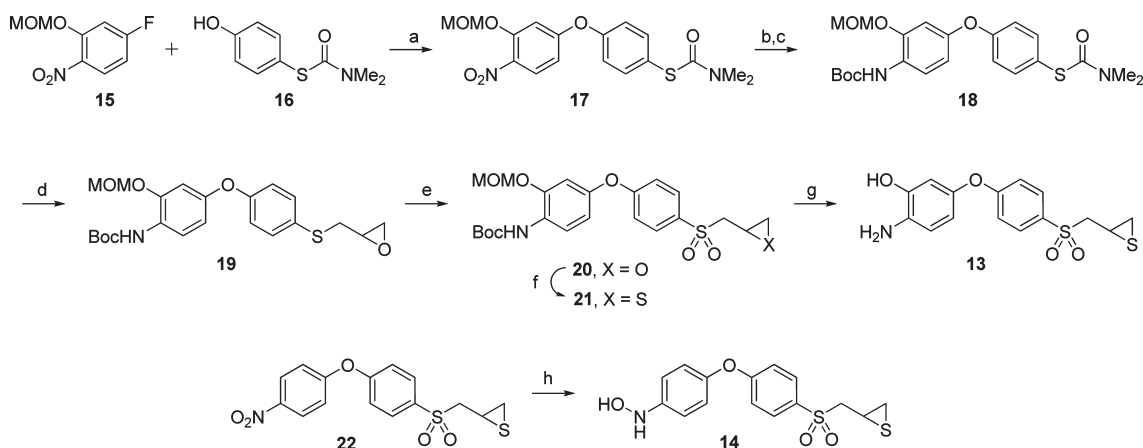
[a] Reagents and conditions: (a) Cs$_2$CO$_3$, DMF, room temperature, 24 h, 88%. (b) Fe, NH$_4$Cl, MeOH/H$_2$O, reflux, 2 h, 83%. (c) Boc$_2$O, Et$_3$N, MeOH, room temperature, 24 h, 76%. (d) KOH, MeOH, reflux, 4 h; then epichlorohydrin, room temperature, 10 min, 68%. (e) m-CPBA, CH$_2$Cl$_2$, 0 °C to room temperature, 10 min, 89%. (f) Thiourea, MeOH/CH$_2$Cl$_2$, room temperature, 24 h, 83%. (g) HCl, MeOH, reflux, 1 h, 95%. (h) Zn, NH$_4$Cl, CH$_2$Cl$_2$/H$_2$O, room temperature, 0.5 h, 69%.
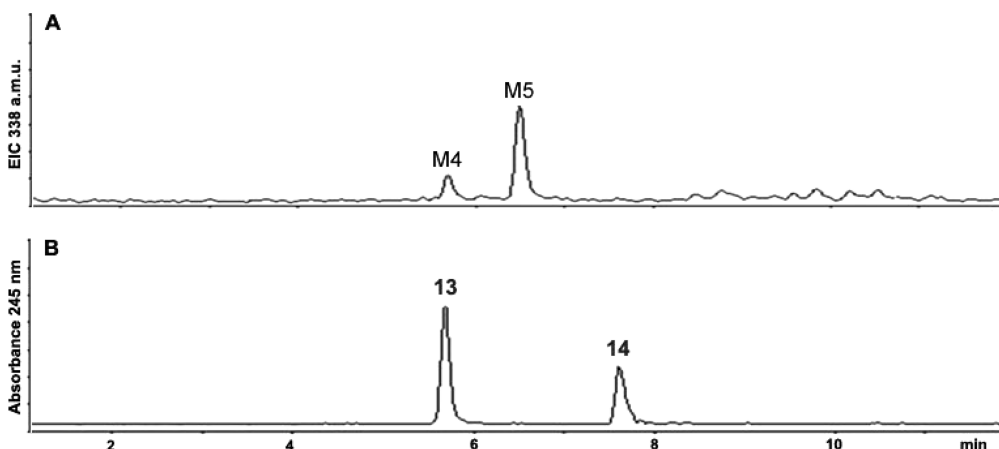
Figure 5. Identification of M4 by comparison of HPLC retention time to synthetic standards. (A) Reconstructed ion chromatogram of m/z 338 following a 30-min incubation of **3** with rat liver microsomes and (B) HPLC chromatogram of a mixture of synthetic standards **13** and **14** using UV absorbance at 245 nm.

N-hydroxylamine derivative **14**. These data conclusively identified metabolite M4 as compound **13**.

The metabolism pathway for **5d** is summarized in Figure 7. Prodrug **5d** is hydrolyzed to the active gelatinase inhibitor **3** as the major biotransformation. A minor metabolism pathway of **5d** and **3** is the oxidation at the α-methylene to give rise to the sulfinic acids M1 and M2. In another minor pathway, the gelatinase inhibitor **3** is oxidized at the terminal phenyl ring to the 3-hydroxy analog **13**. N-Oxidation of the aromatic amine of **3** to N-hydroxylamine **14** does not take place.

Exploration of Potential Toxicity. Aromatic amines could be toxic due to the oxidation by cytochromes P450 to reactive N-hydroxylamine derivatives, which can be conjugated with DNA and proteins or oxidized to nitrosoarenes, which are reactive entities in their own right.[33] These undesired reactivities could result in toxicity and mutagenicity. While **3** contains an aromatic amine, we know definitively from the foregoing experiments that it is not oxidized to the corresponding N-hydroxylamine derivative **14** in vitro. To confirm that the N-hydroxylamine

derivative (compound **14**) is not generated in vivo, we dosed mice with **5d** or **3** and screened plasma and urine samples for the presence of compound **14**. The HPLC and mass spectrometry experiments, along with the direct comparison to the authentic synthetic sample, documented the absence of **14** in vivo.

Notwithstanding the total absence of evidence for the existence of the N-hydroxylamine derivative **14**, we also investigated the potential mutagenicity of both **5d** and **3** by the Ames II mutagenicity test.[34] This assay evaluates the mutagenic potential of a compound by measuring its ability to induce reverse mutations at selected loci of Salmonella typhimurium mixed and tester strains in the presence and absence of rat S9 liver activation (see Experimental Section). The mixed strain contains an equimolar mixture of six strains, which are individually designed to revert by only one specific base-pair substitution. Thus, when mixed, all base-pair mutations are represented in one culture. The tester strain is used to detect frame-shift mutations. Both **5d** and **3** gave negative (nonmutagenic) responses in the Ames II mutagenicity assay with and without S9 metabolic activation up to concentrations of 1 mg/mL (equivalent to 1.8 and
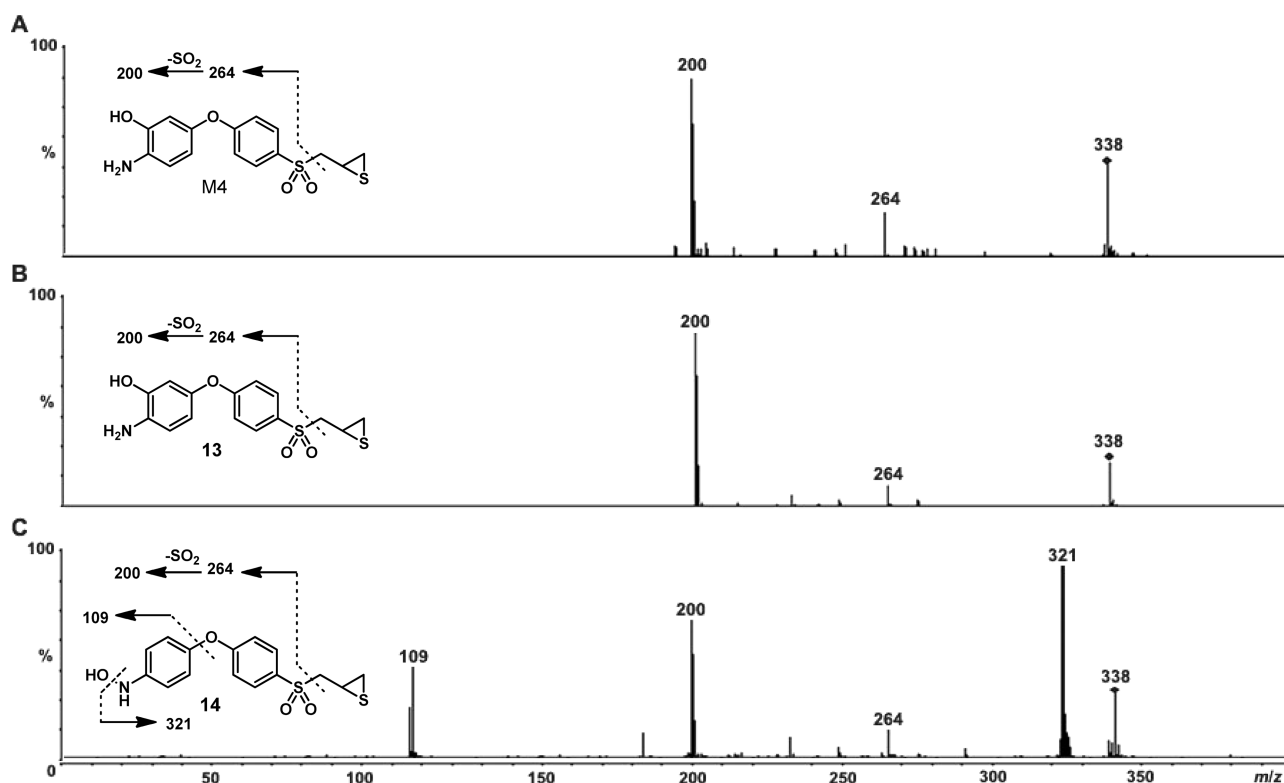
Figure 6. Product ion mass spectra of (A) metabolite M4, (B) synthetic standard **13**, and (C) synthetic standard **14**.
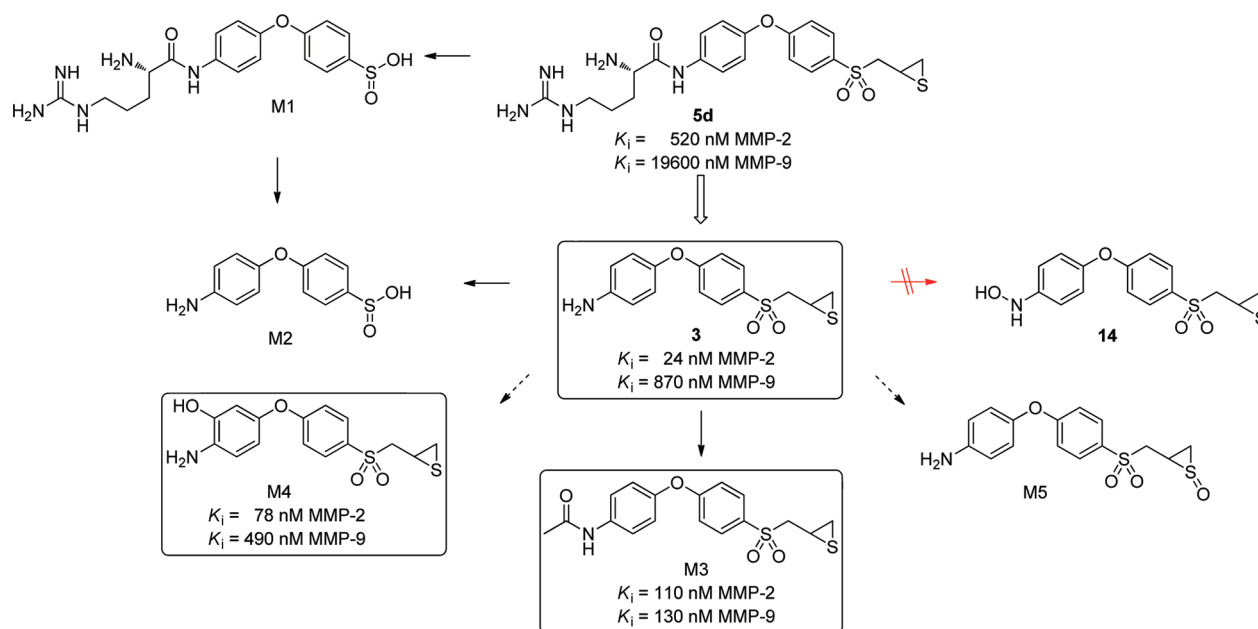

Figure 7. Metabolism pathway of **5d**. Active gelatinase inhibitors are boxed; the major pathway is represented by a thick arrow, minor pathways are depicted by thin arrows, and minute pathways are represented by broken thin arrows. The crossed red arrow indicates the absence of **14**.

2.8 mM of **5d** and **3**, respectively). These results substantiate the nonmutagenic and nontoxic properties of the prodrug **5d**, as well as the active gelatinase inhibitor **3**.

MMP Selectivity. The arginyl amide prodrug **5d** and **3** were evaluated for selectivity toward inhibition of MMPs. Although **5d** showed slow-binding behavior against MMP-14$_{cat}$, its high K_i of

$28.9 \pm 2.3\ \mu$M essentially renders it inactive against the enzyme (Table 5). Furthermore, **5d** was an extremely poor linear competitive inhibitor of MMP-1$_{cat}$, MMP-3$_{cat}$, and MMP-7. As with gelatinases, **3** also showed good slow-binding inhibition of MMP-14$_{cat}$ with a K_i of $0.21 \pm 0.02\ \mu$M. MMP-14 is the cell surface activator of pro-MMP-2,[35] cleaving the *N*-terminal

Table 5. Kinetic Parameters for the Inhibition of MMPs

	$10^{-3} k_{on}$ $(M^{-1} s^{-1})$	$10^4 k_{off}$ (s^{-1})	K_i (μM)
Prodrug 5d			
MMP-14[a]	0.042 ± 0.001	12.0 ± 0.1	28.9 ± 2.3
MMP-1[a]			43% inhibition at 1 mM
MMP-3[a]			40.5 ± 1.2
MMP-7			160 ± 14
Compound 3			
MMP-14[a]	6.0 ± 0.5	12.7 ± 0.8	0.21 ± 0.02
MMP-1[a]			10% inhibition at 250 μM
MMP-3[a]			23.4 ± 1.6
MMP-7			16% inhibition at 250 μM
Compound 13 (M4)			
MMP-2	1.7 ± 0.1	1.4 ± 0.7	0.078 ± 0.043
MMP-9[a]	1.1 ± 0.1	5.3 ± 1.0	0.49 ± 0.11
MMP-14[a]	2.7 ± 0.3	7.0 ± 1.6	0.26 ± 0.07
MMP-1[a]			11% inhibition at 300 μM
MMP-3[a]			54% inhibition at 300 μM
MMP-7			116 ± 13
M3			
MMP-2	1.2 ± 0.3	1.3 ± 0.3	0.11 ± 0.04 [b]
MMP-9			0.13 ± 0.01[b]
MMP-14			0.68 ± 0.05[b]
MMP-1			5.4 ± 0.4 [b]
MMP-3			12.2 ± 0.9 [b]
MMP-7			39 ± 3 [b]

[a] Catalytic domains. [b] Reported earlier and given here for the sake of side-by-side comparison.[28]

prodomain of pro-MMP-2 and generating the activated intermediate, which matures into the fully active form of MMP-2.[36] However, **3** extremely poorly inhibited MMP-1$_{cat}$, MMP-3$_{cat}$, and MMP-7.

As observed for the sulfinic acid and sulfoxide derivatives of **1**,[21] the minor sulfinic acid metabolites of **5d**, M1 and M2, as well as the sulfoxide M5, are also expected to be poor inhibitors of gelatinases, as the critical thiirane warhead in these compounds is missing. The *N*-acetyl metabolite (M3) is, however, a potent inhibitor of gelatinases.[28] Compound **13** (M4) was also tested for inhibitory activities toward MMPs. It displayed a slow-binding inhibition profile similar to that of **3**, with inhibition constants (K_i) of 0.078 ± 0.043, 0.49 ± 0.11, and 0.26 ± 0.07 μM for MMP-2, MMP-9$_{cat}$, and MMP-14$_{cat}$, respectively, while sparing MMP-1$_{cat}$, MMP-3$_{cat}$, and MMP-7 (Table 5). The concept of the prodrug strategy is well demonstrated by **5d**, which is hydrolyzed in the bloodstream to the active **3**, which, in turn, gets further metabolized to two additional minor metabolites, M3 and M4, both of which are potent gelatinase inhibitors in their own right. Note that while M4 was detected as a minor metabolite in vitro, it was not observed in vivo.

Pharmacokinetics. The pharmacokinetics of **5d** and **3** were separately evaluated in mice, following a single bolus intravenous dose administration at 12.5 mg/kg. Concentrations of **5d**, **3**, and the *p-N*-acetyl derivative (M3) are summarized in Table 6. We did not determine the blood levels of the other metabolites because their concentrations were quite low, including M4, which was not observed in the plasma. As predicted from the ex vivo experiments, administration of **5d** to mice resulted in hydrolysis to **3**, which further metabolized to the *p-N*-acetyl derivative (M3). Pharmacokinetic parameters are calculated in Table 6.

Following intravenous administration of **5d**, plasma levels of **5d** were initially 198 μM and declined rapidly, with a $t_{1/2\alpha}$ (distribution half-life) of less than 1 min and a longer elimination half-life ($t_{1/2\beta}$) of >4 h. Systemic exposure (AUC) of **5d** was 363 μM·min. The calculated clearance (CL) of 0.0582 L/min/kg was lower than the hepatic blood flow of 0.086 L/min/kg,[31] indicating moderate clearance of the prodrug from systemic circulation. The volume of distribution (Vd) of 0.0978 L/kg (equivalent to 2.30 mL) was significantly lower than the total body water of 14.5 mL,[31] suggesting that **5d** was poorly distributed to tissues and remained primarily in the extracellular fluid compartment. The low volume of distribution for the prodrug **5d** was attributed to the fact that this compound was designed to be readily hydrolyzed to **3** by amidases present in blood. Thus, **5d** is not anticipated to be distributed to tissues and is expected to remain in the extracellular fluid compartment, as was found experimentally. This is consistent with prodrugs that are readily hydrolyzed in blood to the active drugs[37,38] and have volumes of distribution significantly lower than total body water. For example, fospropofol is a phosphate ester water-soluble prodrug which is readily hydrolyzed to propofol in blood. Fospropofol shows a Vd of 0.25 L/kg in rats and 0.11 L/kg in humans, while propofol has a Vd of 2.3 L/kg in rats and 12.4 L/kg in humans.[37,38] Systemic exposure of **3** was 138 μM·min, 2.6-fold lower than that of **5d**. The terminal half-life of **3** was 69 min or 3-fold shorter than that of **5d**. The *p-N*-acetyl derivative (M3), generated from *N*-acetylation of **3**, had a distribution half-life of 12 min and a systemic exposure of 4.22 μM·min, which was significantly lower (33-fold) than the systemic exposure of **3**. This is consistent with the observation of *N*-acetylation as a minor metabolism pathway. Mice that received **5d** had quantifiable levels of both the prodrug and the released active constituent **3** up to 4 h postadministration of **5d**.

In contrast, intravenous administration of **3** resulted in initial plasma levels of 36.4 μM and systemic exposure of 221 μM·min. The terminal half-life of 21 min was considerably shorter than that of **3** generated from the administration of **5d**. Clearance of 0.0875 L/min/kg was >70% hepatic blood flow of 0.086 L/min/kg,[31] indicating high clearance of **3**. The volume of distribution was 0.532 L/kg (equivalent to 12.5 mL) and approximated total body water of 14.5 mL, indicating that **3** was distributed to the tissues. Moreover, the resulting *p-N*-acetyl metabolite (M3) had an initial half-life of 5.1 min, 2.4-fold shorter than that generated after the administration of **5d**. Systemic exposure of 7.71 μM·min, 29-fold lower than that of **3**, further indicated that *N*-acetylation was a minor metabolism pathway and/or that the *p-N*-acetyl metabolite was cleared from systemic circulation.

Comparison of the blood levels of **3** after a single bolus intravenous administration of **5d** and **3** to mice is shown graphically in Figure 8. More favorable pharmacokinetic properties were observed following intravenous administration of **5d** than **3**. In particular, the terminal half-life of **3** generated from **5d** was more than 3-fold longer than that after the administration of **3** itself. The in vivo pharmacokinetic data were consistent with the in vitro results and indicated that **5d** had superior pharmacokinetic properties compared to those of **3**. The >4 h elimination half-life for **5d** indicates that this prodrug can be administered as an

Table 6. Pharmacokinetic Parameters of 5d and 3 after a Single Bolus Intravenous Dose to Mice

time (min)	IV dose of 5d			IV dose of 3	
	5d (μM)	3 (μM)	M3 (μM)	3 (μM)	M3 (μM)
0	198	25.7		36.4	
2−3	35.1 ± 9.65	12.3 ± 3.79	0.0354 ± 0.0184	18.4 ± 3.56	0.197 ± 0.0616
4−5	7.32 ± 5.76	10.4 ± 2.31	0.231 ± 0.0197	13.4 ± 3.29	0.462 ± 0.313
7−8	1.28 ± 0.0544	4.50 ± 0.361	0.176 ± 0.0913	5.33 ± 0.863	0.192 ± 0.0121
11−12	1.58 ± 0.423	2.45 ± 0.664	0.149 ± 0.0243	3.44 ± 0.775	0.150 ± 0.0272
22	0.138 ± 0.0451	0.787 ± 0.373	0.0627 ± 0.0169		
30				1.11 ± 1.11	0.0958 ± 0.0830
42	0.0872 ± 0.00313	0.207 ± 0.0388	0.0358 ± 0.0178		
62−66	0.0385 ± 0.00582	0.0908 ± 0.0403	0.0121 ± 0.00181	0.138 ± 0.0609	0.0273 ± 0.00628
120−123	0.0171 ± 0.00652	0.0248 ± 0.00652	NQ[a]	0.0190 ± 0.00350	0.00277 ± 0.00480
240	0.00830 ± 0.00820	0.0145 ± 0.00573	NQ[g]	NQ[a]	NQ[a]
AUC_{0-last} (μM·min)	360	137	4.22	221	7.71
$AUC_{0-\infty}$ (μM·min)	363	138	NC[b]	221	NC[b]
CL (L/min/kg)	0.0582			0.0875	
Vd (L/kg)	0.0978			0.532	
$t_{1/2\alpha}$ (min)	0.88	2.9	12	3.0	5.1
$t_{1/2\beta}$ (min)	260	69	NC[b]	21	NC[b]

[a] NQ = not quantifiable. [b] NC = not calculated because the low levels observed did not allow for the calculation of the terminal half-life and $AUC_{last-\infty}$.

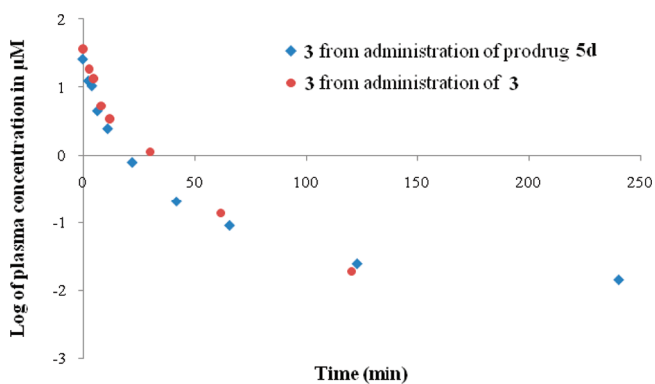**Figure 8.** Plasma concentration−time curves of 3 after a single bolus intravenous dose of 5d and 3 to mice.

intravenous infusion, which is the preferred route of administration in the treatment of acute gelatinase-dependent diseases, such as stroke, aneurysm, and traumatic brain injury.

Plasma levels of 3 remained above the K_i for MMP-2 for 2 h and were higher than the K_i for MMP-9 for 20 min. However, we had previously demonstrated that the mechanism of inhibition of the thiirane class of gelatinase inhibitors is a rate-limiting gelatinase-mediated generation of a thiolate within the enzyme active site.[12] Once the thiolate is generated, it has significantly tighter binding than the parental thiirane, as documented for the prototype 1, which shows a 26-fold more potent inhibition of MMP-2 compared to the thiirane (K_i of 530 pM for the thiolate versus 14 nM for the thiirane).[12] The ability of gelatinases to perform this chemistry within the active site is the reason for the selectivity that this class of inhibitors enjoys in the inhibition of gelatinases. Similarly, once 3 is generated from 5d in vivo, we anticipate that on binding to the active site of gelatinases, the same chemistry leads to the formation of the tight-binding thiolate that ties up the enzyme in manifestation of the biological activity of this class of compounds in vivo.

■ CONCLUSION

Gelatinases are important targets of inhibition in many diseases, in particular acute neurological conditions such as stroke, aneurysm, and traumatic brain injury. For treatment of these diseases, intravenous infusion is the preferred route of administration, which requires a drug to possess a water solubility of 10 mg/mL. We addressed the poor water solubility and extensive metabolism of the prototype thiirane inhibitor 1 by blocking the primary site of metabolism and capitalizing on a prodrug strategy. The prodrugs increased aqueous solubility by more than 5000-fold. The amide prodrugs were quantitatively hydrolyzed in human blood to a potent and selective gelatinase inhibitor. The arginyl amide prodrug 5d was metabolically stable in mouse, rat, and human liver microsomes. The major metabolism pathway of 5d was hydrolysis to the corresponding p-amino derivative 3; minor pathways were N-acetylation, oxidation at the terminal phenyl ring, and oxidation at the α-methylene. Both N-acetylation and hydroxylation at the terminal phenyl ring generated active gelatinase inhibitors. N-Hydroxylation of the aromatic amine was not observed in vitro or in vivo. Both 5d and 3 were nonmutagenic in the Ames II mutagenicity assay. Following a single intravenous bolus administration of 5d to mice, systemic exposures of 5d, 3, and the p-N-acetyl derivative were 363, 138, and 4.22 μM·min, respectively. The prodrug 5d showed a moderate clearance of 0.0582 L/min/kg, remained mostly in the extracellular fluid compartment (Vd = 0.0978 L/kg), and had a moderate terminal half-life of >4 h. The prodrug 5d had superior pharmacokinetic properties compared to those of 3. The high water solubility, chemical stability, quantitative enzymatic hydrolysis of the amide prodrugs, metabolic stability, lack of toxicity, and favorable pharmacokinetic properties make the

thiirane class of selective gelatinase inhibitors suitable for intravenous administration in the treatment of acute gelatinase-dependent diseases.

■ EXPERIMENTAL SECTION

Chemistry. Organic reagents and solvents were purchased from either Sigma-Aldrich Chemical Co. (St. Louis, MO, USA) or Acros Organics (Geel, Belgium), unless otherwise stated, and were used without further purification. All reactions were performed under an atmosphere of nitrogen, unless noted otherwise. ^{1}H and ^{13}C NMR spectra were recorded on a Varian INOVA-500 (Varian Inc., Palo Alto, CA, USA) or a Varian DirectDrive 600 spectrometer (Varian Inc., Palo Alto, CA, USA). Thin-layer chromatography was performed with Whatman reagents 0.25 mm silica gel 60-F plates. Flash chromatography was carried out with silica gel 60, 230−400 mesh (0.040−0.063 mm particle size) purchased from EM Science (Gibbstown, NJ, USA). High-resolution mass spectra were obtained at the Department of Chemistry and Biochemistry, University of Notre Dame by FAB ionization, using a JEOL AX505HA mass spectrometer (Tokyo, Japan) or ESI ionization, using a Bruker micrOTOF/Q2 mass spectrometer (Bruker Daltonik, Bremen, Germany). Purity of the prepared compounds was generally >95%, confirmed by HPLC. Detailed conditions are given in the HPLC section.

t-Butyl [4-(4-allylthiophenoxy)phenyl]carbamate (9). Compound **8** (10.3 g, 40.0 mmol), which was prepared by a literature method,[28] was dissolved in a mixture of MeOH and triethylamine (7:1, 80 mL), and di-*t*-butyl dicarbonate (17.5 g, 80 mmol) was added. The resulting solution was stirred for 2 h at 60 °C and was concentrated under reduced pressure. The crude material was purified by column chromatography on silica gel to give the title compound (11.7 g, 82%). ^{1}H NMR (600 MHz, CDCl$_3$) δ 1.53 (s, 9H), 3.48 (d, J = 6.7 Hz, 2H), 4.96−5.09 (m, 2H), 5.86 (m, J = 16.7, 10.3 Hz, 1H), 6.47 (br. s, 1H), 6.89 (d, J = 8.8 Hz, 2H), 6.96 (d, J = 8.8 Hz, 2H), 7.24−7.39 (m, 4H); ^{13}C NMR (151 MHz, CDCl$_3$) δ 28.5, 38.9, 80.7, 117.7, 118.6, 120.3, 120.5, 128.9, 133.3, 134.0, 134.5, 152.2, 153.1, 157.4. HRMS-FAB (m/z): [M]$^+$, calcd for C$_{20}$H$_{23}$NO$_3$S, 357.1399; found, 357.1402.

t-Butyl [4-(4-((Thiiran-2-yl)methylsulfonyl)phenoxy)phenyl] carbamate (10). To a solution of compound **9** (10.0 g, 28.0 mmol) in CH$_2$Cl$_2$ (100 mL) was added a solution of m-CPBA (31.2 g, 140 mmol, 77%) in an ice−water bath. After 72 h, the suspension was filtered, and the filtrate was diluted with EtOAc and washed with 10% aqueous sodium thiosulfate, followed by washes with saturated sodium bicarbonate and brine. The organic layer was dried over MgSO$_4$ and was concentrated. The product was purified by silica gel chromatography to yield the oxirane (7.4 g, 81%) with recovery of some of the allylsulfone derivative (2.1 g, 19%). ^{1}H NMR (600 MHz, CDCl$_3$) δ 1.50 (s, 9H), 2.45 (dd, J = 5.0, 1.2 Hz, 1H), 2.79 (dd, J = 4.4, 2.6 Hz, 1H), 3.24−3.34 (m, 3H), 6.85 (s, 1H), 6.99 (d, J = 8.8 Hz, 2H), 7.02 (d, 2H), 7.42 (d, J = 8.2 Hz, 2H), 7.84 (d, J = 8.8 Hz, 2H); ^{13}C NMR (151 MHz, CDCl$_3$) δ 28.4, 46.0, 46.0, 59.7, 117.2, 120.5, 121.3, 130.6, 132.2, 136.0, 149.8, 153.0, 163.4. HRMS-FAB (m/z): [M]$^+$, calcd for C$_{20}$H$_{23}$NO$_6$S, 405.1246; found, 405.1230.

Thiourea (2.4 g, 31.5 mmol) was added to a solution of the oxirane (6.0 g, 14.8 mmol), obtained above, in a 1:1 mixture of methanol and CH$_2$Cl$_2$ (50 mL). The reaction mixture was stirred at room temperature for 18 h. The solvent was removed under reduced pressure. The residue was partitioned between CH$_2$Cl$_2$ and water, the organic layer was washed with brine and water and dried (MgSO$_4$), and the suspension was filtered. Evaporation of solvent gave the crude product, which was purified by column chromatography on silica gel to give thiirane **10** (4.4 g, 72%). ^{1}H NMR (600 MHz, CDCl$_3$) δ 1.53 (s, 9H), 2.16 (dd, J = 5.1, 1.6 Hz, 1H), 2.54 (dd, J = 6.2, 1.2 Hz, 1H), 3.06 (dq, J = 7.6, 5.7 Hz, 1H), 3.17 (dd, J = 14.1, 7.9 Hz, 1H), 3.53 (dd, J = 14.1, 5.6 Hz, 1H), 6.61 (br. s, 1H), 7.06 (d, J = 8.8 Hz, 2H), 7.03 (d, J = 8.8 Hz, 2H), 7.44 (d, J = 8.5 Hz, 2H), 7.84 (d, J = 8.8 Hz, 2H); ^{13}C NMR (151 MHz, CDCl$_3$)

δ 24.5, 26.3, 28.5, 62.8, 81.0, 117.4, 120.6, 121.4, 130.9, 131.8, 136.0, 150.0, 153.0, 163.6. HRMS-FAB (m/z): [M]$^+$, calcd for C$_{20}$H$_{23}$NO$_5$S$_2$, 421.1018; found, 421.1009.

4-[4-((Thiiran-2-yl)methylsulfonyl)phenoxy]benzanmine · HCl Salt (3). The thiirane (**10**, 4.0 g, 9.5 mmol) was dissolved in a 1:1 mixture of CH$_2$Cl$_2$ and ethyl acetate (40 mL), and HCl (10 mL, 4 N in dioxane) was added. The reaction mixture was stirred for 48 h and concentrated under reduced pressure. The resulting crude compound was triturated with diethyl ether, and the product was obtained by filtration (2.8 g, 82%). ^{1}H NMR (500 MHz, D$_2$O) δ 2.03 (d, J = 4.8 Hz, 1H), 2.42 (d, J = 6.4 Hz, 1H), 2.94 (m, J = 6.4, 6.4 Hz, 1H), 3.42 (dd, J = 14.4, 6.4 Hz, 1H), 3.61 (dd, J = 14.4, 6.4 Hz, 1H), 7.11 (d, J = 8.0 Hz, 2H), 7.16 (d, J = 8.0 Hz, 2H), 7.35 (d, J = 8.0 Hz, 2H), 7.80 (d, J = 8.0 Hz, 2H); ^{13}C NMR (126 MHz, D$_2$O) δ 23.5, 26.0, 61.4, 118.6, 121.9, 125.2, 126.8, 130.8, 131.1, 155.2, 162.5. HRMS-FAB (m/z): [M + H]$^+$, calcd for C$_{15}$H$_{16}$NO$_3$S$_2$, 322.0572; found, 322.0569.

Syntheses of Ester Prodrugs (4). Synthesis of the lysine prodrug (**4b**) is given here as a representative example. To a solution of **2** (0.20 g, 0.62 mmol) in CH$_2$Cl$_2$ (5 mL), which was prepared by a literature method,[23] was added N_α, N_ε-di-Boc-L-lysine hydroxysuccinimide ester (0.41 g, 0.93 mmol) at room temperature. DMAP (76 mg, 0.62 mmol) and diisopropylethyl amine (108 uL, 0.62 mmol) were added, and the reaction mixture was stirred for 3 h at room temperature. After concentrating the solution under reduced pressure, the crude product was purified by column chromatography on silica gel to give the desired product (**11b**, 0.30 g, 74%). The ester (0.30 g, 0.46 mmol) was dissolved in CH$_2$Cl$_2$ and ethyl acetate (1:1, 4 mL), and HCl (2 mL, 4 N in dioxane) was added. The reaction mixture was stirred for 48 h and was concentrated under reduced pressure. The resulting crude compound was triturated with diethyl ether, and the product (**4b**) was obtained by filtration (0.18 g, 75%).

Syntheses of Amide Prodrugs (5). Synthesis of the lysine prodrug (**5b**) is shown as a representative example. i-Butylchloroformate (83 µL, 0.53 mmol) was added to a mixture of $N_\alpha N_\varepsilon$-di-Boc-L-lysine dicyclohexylamine salt (0.28 g, 0.64 mmol) and N-methylmorpholine (140 µL, 1.3 mmol) in THF (4 mL) at −15 °C. After stirring for 0.5 h at the same temperature, the suspension of **3** (0.19 g, 0.53 mmol) and N-methylmorpholine (58 µL, 0.53 mmol) in THF (2 mL) was added to the reaction mixture. Stirring was continued for 1 h, while the temperature was gradually increased to room temperature. The reaction mixture was diluted with CH$_2$Cl$_2$/water, and layers were separated. The aqueous layer was washed with CH$_2$Cl$_2$, and the combined organic layer was dried (MgSO$_4$) and evaporated to dryness. The crude material was purified by column chromatography on silica gel to afford the desired product (**12b**, 0.21 g, 64%). The amide (0.20 g, 0.30 mmol) was dissolved in CH$_2$Cl$_2$ and ethyl acetate (1:1, 3 mL), and HCl (2 mL, 4 N in dioxane) was added. The reaction mixture was stirred for 48 h and concentrated under reduced pressure. The resulting crude compound was triturated with diethyl ether, and the product (**5b**) was obtained by filtration (0.11 g, 71%).

Spectral Data of Gly Ester Prodrug Compound 11a. ^{1}H NMR (500 MHz, CDCl$_3$) δ 1.48 (s, 9H), 2.17 (dd, J = 5.0, 1.8 Hz, 1H), 2.55 (dd, J = 6.2, 1.8 Hz, 1H), 3.04−3.10 (m, 1H), 3.20 (dd, J = 14.4, 7.8 Hz, 1H), 3.52 (dd, J = 14.2, 5.6 Hz, 1H), 4.19 (d, J = 5.8 Hz, 2H), 7.11 (d, J = 9.0 Hz, 2H), 7.12 (d, J = 8.8 Hz, 2H), 7.18 (d, J = 9.0 Hz, 2H), 7.88 (d, J = 9.0 Hz, 2H); ^{13}C NMR (126 MHz, CDCl$_3$) δ 24.4, 26.2, 28.5, 42.7, 62.7, 80.5, 117.9, 121.5, 123.3, 131.0, 132.4, 147.3, 152.6, 162.8, 169.3. HRMS-ESI (m/z): [M + H]$^+$, calcd for C$_{22}$H$_{26}$N$_2$O$_6$S$_2$, 480.1145; found, 480.1145. Compound **4a**: ^{1}H NMR (500 MHz, D$_2$O) δ 2.17 (dd, J = 5.2, 1.2 Hz, 1H), 2.56 (d, J = 6.2 Hz, 1H), 3.09 (quin, J = 6.2 Hz, 1H), 3.57 (dd, J = 14.6, 7.2 Hz, 1H), 3.74 (dd, J = 14.6, 6.4 Hz, 1H), 4.25 (s, 2H), 7.21−7.35 (m, 6H), 7.93 (d, J = 8.8 Hz, 2H). HRMS-ESI (m/z): [M + H]$^+$, calcd for C$_{17}$H$_{18}$NO$_5$S$_2$, 380.0621; found, 380.0597.

Spectral Data of Lys Ester Prodrug Compound **11b**. ^{1}H NMR (500 MHz, CDCl$_3$) δ 1.45 (s, 9H), 1.47 (s, 9H), 1.52 (m, 2H), 1.56 (m, 4H), 1.85 (m, 1H), 1.99 (m, 1H), 2.17 (dd, J = 5.2, 1.8 Hz, 1H), 2.55 (dd, J = 6.2, 1.8 Hz, 1H), 3.07 (m, 1H), 3.17 (m, 2H), 3.19 (dd, J = 14.2, 7.8 Hz, 1H), 3.53 (dd, J = 14.2, 5.6 Hz, 1H), 4.49 (m, 1H), 4.61 (m, 1H), 5.23 (d, J = 7.4 Hz, 1H), 7.10 (d, J = 9.0 Hz, 1H), 7.11 (d, J = 8.8 Hz, 2H), 7.17 (d, J = 9.0 Hz, 1H); ^{13}C NMR (126 MHz, CDCl$_3$) δ 22.7, 24.4, 26.3, 28.5, 28.6, 29.9, 32.1, 40.1, 53.8, 62.8, 79.5, 80.3, 81.3, 117.9, 121.6, 123.4, 131.0, 132.4, 147.6, 152.6, 162.9, 171.8. HRMS-ESI (m/z): [M + H]$^+$, calcd for C$_{31}$H$_{43}$N$_2$O$_9$S$_2$, 651.2404; found, 651.2414. Compound **4b**: ^{1}H NMR (500 MHz, 10% CDCl$_3$ in CD$_3$OD) δ 1.62−1.84 (m, 4H), 2.05−2.26 (m, 2H), 2.14 (dd, J = 5.0, 1.4 Hz, 1H), 2.52 (dd, J = 6.3, 1.1 Hz, 1H), 3.01 (t, J = 7.6 Hz, 2H), 3.06 (m, 1H), 3.46 (dd, J = 14.6, 7.0 Hz, 1H), 3.54 (t, J = 6.6 Hz, 1H), 4.40 (t, J = 6.5 Hz, 1H), 7.19 (d, J = 9.0 Hz, 2H), 7.23 (d, J = 9.0 Hz, 2H), 7.32 (d, J = 9.2 Hz, 2H), 7.94 (d, J = 9.0 Hz, 2H). HRMS-ESI (m/z): [M + H]$^+$, calcd for C$_{21}$H$_{27}$N$_2$O$_5$S$_2$, 451.1356; found, 541.1298.

Spectral Data of Glu Ester Prodrug Compound **11c**. ^{1}H NMR (500 MHz, CDCl$_3$) δ 1.45 (s, 18H), 2.09 (m, 1H), 2.15 (dd, J = 5.2, 1.8 Hz, 1H), 2.29 (m, 1H), 2.43 (q, J = 7.4 Hz, 2H), 2.52 (dd, J = 6.2, 1.8 Hz, 1H), 3.05 (m, 1H), 3.18 (dd, J = 14.4, 7.8 Hz, 1H), 3.51 (dd, J = 14.4, 5.8 Hz, 1H), 4.52 (m, 1H), 5.26 (d, J = 8.2 Hz, 1H), 7.08 (d, J = 9.0 Hz, 2H), 7.09 (d, J = 9.0 Hz, 2H), 7.17 (d, J = 9.2 Hz, 2H), 7.86 (d, J = 9.0 Hz, 2H); ^{13}C NMR (126 MHz, CDCl$_3$) δ 24.4, 26.2, 27.3, 28.2, 28.4, 31.7, 53.5, 62.7, 80.4, 81.1, 117.9, 121.4, 123.3, 130.9, 132.3, 147.5, 152.5, 155.6, 162.8, 171.3, 172.1. HRMS-ESI (m/z): [M + H]$^+$, calcd for C$_{29}$H$_{38}$NO$_9$S$_2$, 608.1982; found, 608.1981. Compound **4c**: ^{1}H NMR (500 MHz, 10% CDCl$_3$ in CD$_3$OD) δ 2.14 (dd, J = 5.1, 1.3 Hz, 1H), 2.37 (m, 2H), 2.52 (dd, J = 6.2, 1.0 Hz, 1H), 2.68 (td, J = 7.1, 1.6 Hz, 2H), 3.05 (quin, J = 6.2 Hz, 1H), 3.44 (dd, J = 14.4, 7.0 Hz, 1H), 3.54 (dd, J = 14.4, 6.4 Hz, 1H), 4.43 (t, J = 6.8 Hz, 1H), 7.19 (d, J = 8.8 Hz, 2H), 7.22 (d, J = 9.2 Hz, 2H), 7.32 (d, J = 9.0 Hz, 2H), 7.93 (d, J = 9.0 Hz, 2H). HRMS-ESI (m/z): [M + H]$^+$, calcd for C$_{20}$H$_{22}$NO$_7$S$_2$, 452.0832: found, 452.0769.

Spectral Data of Arg Ester Prodrug Compound **11d**. ^{1}H NMR (500 MHz, CDCl$_3$) δ 1.46 (s, 9H), 1.50 (s, 9H), 1.77 (m, 1H), 1.94 (m, 1H), 2.13 (dd, J = 5.0, 1.6 Hz, 1H), 2.51 (dd, J = 6.2, 1.6 Hz, 1H), 3.03 (m, 1H), 3.17 (dd, J = 14.2, 7.8 Hz, 1H), 3.49 (dd, J = 14.2, 5.6 Hz, 1H), 3.84 (m, 1H), 3.96 (m, 1H), 4.50 (m, 1H), 5.83 (d, J = 8.2 Hz, 1H), 7.07 (d, J = 9.0 Hz, 2H), 7.08 (d, J = 8.8 Hz, 2H), 7.14 (d, J = 9.0 Hz, 1H), 7.85 (d, J = 9.0 Hz, 2H); ^{13}C NMR (126 MHz, CDCl$_3$) δ 24.3, 26.2, 28.1, 28.3, 28.5, 44.1, 53.5, 60.5, 62.7, 84.1, 117.8, 121.4, 123.4, 130.9, 132.3, 147.7, 152.4, 155.0, 155.6, 160.6, 162.8, 163.6, 171.2. HRMS-ESI (m/z): [M + H]$^+$, calcd for C$_{36}$H$_{51}$N$_4$O$_{11}$S$_2$, 779.2990; found, 779.3001. Compound **4d**: ^{1}H NMR (500 MHz, 10% CDCl$_3$ in CD$_3$OD) δ 1.78−2.26 (m, 4H), 2.14 (dd, J = 5.1, 1.3 Hz, 1H), 2.52 (dd, J = 6.2, 0.8 Hz, 1H), 3.04 (quin, J = 6.2 Hz, 1H), 3.27 (m, 2H), 3.43 (dd, J = 14.4, 7.0 Hz, 1H), 3.52 (dd, J = 14.8, 6.6 Hz, 1H), 4.39 (t, J = 6.5 Hz, 1H), 7.17 (d, J = 9.0 Hz, 1H), 7.21 (d, J = 9.0 Hz, 1H), 7.30 (d, J = 9.0 Hz, 2H), 7.92 (d, J = 8.8 Hz, 2H). HRMS-ESI (m/z): [M + H]$^+$, calcd for C$_{21}$H$_{27}$N$_4$O$_5$S$_2$, 479.1417; found, 479.1423.

Spectral Data of Arg-Arg Ester Prodrug Compound **11e**. ^{1}H NMR (500 MHz, CDCl$_3$) δ 1.39−1.53 (m, 45H), 1.54−2.11 (m, 8H), 2.16 (dd, J = 5.2, 1.4 Hz, 1H), 2.54 (d, J = 5.2 Hz, 1H), 3.06 (m, 1H), 3.19 (dd, J = 14.2, 7.8 Hz, 1H), 3.47 (dd, J = 12.8, 7.0 Hz, 2H), 3.52 (dd, J = 14.4, 5.6 Hz, 1H), 3.74−3.95 (m, 2H), 4.32 (dd, J = 14.8, 6.4 Hz, 1H), 4.77 (m, 1H), 5.92 (d, J = 7.8 Hz, 1H), 7.07−7.12 (m, 4H), 7.16 (d, J = 9.0 Hz, 2H), 7.33 (d, J = 7.6 Hz, 1H), 7.87 (d, J = 8.8 Hz, 2H), 8.38 (t, J = 4.9 Hz, 1H), 9.30 (br. s, 2H), 11.50 (s, 1H); ^{13}C NMR (126 MHz, CDCl$_3$) δ 24.4, 24.9, 25.6, 26.2, 28.2, 28.2, 28.5, 28.6, 29.3, 40.4, 44.1, 52.5, 54.3, 62.8, 79.5, 80.2, 83.4, 83.5, 84.2, 117.9, 121.5, 121.5, 123.4, 130.8, 131.0, 132.3, 147.5, 152.5, 153.4, 155.0, 156.4, 160.8, 160.9, 162.9, 163.7, 170.6, 172.7. HRMS-ESI (m/z): [M + H]$^+$, calcd for C$_{52}$H$_{79}$N$_8$O$_{16}$S$_2$, 1135.5050; found, 1135.5039. Compound **4e**: ^{1}H NMR (500 MHz, 10% CDCl$_3$ in

CD$_3$OD) δ 1.71−2.23 (m, 8H), 2.16 (dd, J = 5.0, 1.2 Hz, 1H), 2.54 (dd, J = 6.2, 0.8 Hz, 1H), 3.03−3.10 (m, 1H), 3.23−3.32 (m, 4H), 3.47 (dd, J = 14.4, 7.0 Hz, 1H), 3.54 (dd, J = 14.2, 6.4 Hz, 1H), 4.16 (t, J = 6.4 Hz, 1H), 4.72 (dd, J = 9.1, 4.5 Hz, 1H), 7.15−7.23 (m, 4H), 7.25 (d, J = 9.0 Hz, 2H), 7.94 (d, J = 8.8 Hz, 2H). HRMS-ESI (m/z): [M + H]$^+$, calcd for C$_{27}$H$_{39}$N$_8$O$_6$S$_2$, 635.2428; found, 635.2449.

Spectral Data of Gly Amide Prodrug Compound **12a**. ^{1}H NMR (500 MHz, CDCl$_3$) δ 1.37 (s, 9H), 2.05 (dd, J = 5.2, 1.8 Hz, 1H), 2.44 (dd, J = 6.2, 1.8 Hz, 1H), 2.94 (m, 1H), 3.14 (dd, J = 14.4, 7.6 Hz, 1H), 3.41 (dd, J = 14.4, 6.0 Hz, 1H), 3.80 (d, J = 5.2 Hz, 2H), 3.82 (s, 1H), 6.96 (d, J = 15.2 Hz, 2H), 6.98 (d, J = 15.4 Hz, 2H), 7.52 (d, J = 8.8 Hz, 2H), 7.75 (d, J = 9.0 Hz, 2H); ^{13}C NMR (126 MHz, CDCl$_3$) δ 24.0, 25.9, 28.2, 44.2, 62.5, 80.4, 117.4, 121.0, 121.8, 130.7, 131.4, 150.7, 163.3, 168.3, 172.9. HRMS-ESI (m/z): [M + Na]$^+$, calcd for C$_{22}$H$_{26}$N$_2$O$_6$S$_2$Na, 501.1124; found, 501.1112. Compound **5a**: ^{1}H NMR (500 MHz, 10% CDCl$_3$ in CD$_3$OD) δ 2.14 (dd, J = 5.2, 1.6 Hz, 1H), 2.51 (dd, J = 6.3, 1.5 Hz, 1H), 3.04 (m, J = 7.0, 5.2 Hz, 1H), 3.42 (dd, J = 14.4, 7.0 Hz, 1H), 3.53 (dd, J = 14.4, 6.4 Hz, 1H), 4.14 (s, 2H), 7.17 (d, J = 9.0, 2.0, 1.8 Hz, 1H), 7.20 (d, J = 9.2 Hz, 2H), 7.29 (d, J = 9.2 Hz, 2H), 7.92 (d, J = 9.2 Hz, 1H). HRMS-ESI (m/z): [M + H]$^+$, calcd for C$_{17}$H$_{19}$N$_2$O$_4$S$_2$, 379.0781; found, 379.0805.

Spectral Data of Lys Amide Prodrug Compound **12b**. ^{1}H NMR (500 MHz, CDCl$_3$) δ 1.41 (s, 9H), 1.43 (s, 9H), 2.02 (s, 3H), 2.13 (dd, J = 5.0, 1.6 Hz, 1H), 2.50 (dd, J = 6.2, 1.6 Hz, 1H), 3.02 (m, 1H), 3.09 (m, 2H), 3.16 (dd, J = 14.4, 7.8 Hz, 1H), 3.50 (dd, J = 14.4, 5.8 Hz, 1H), 4.28 (m, 1H), 4.75 (m, 1H), 5.53 (d, J = 7.4 Hz, 1H), 6.93 (d, J = 8.4 Hz, 2H), 7.00 (d, J = 8.6 Hz, 2H), 7.55 (d, J = 8.8 Hz, 2H), 7.82 (d, J = 9.0 Hz, 2H); ^{13}C NMR (126 MHz, CDCl$_3$) δ 24.4, 26.2, 28.5, 28.6, 29.8, 31.9, 39.8, 55.3, 62.7, 79.3, 80.5, 117.4, 121.1, 121.7, 130.8, 131.8, 135.6, 150.5, 156.4, 156.6, 163.3, 171.2. HRMS-ESI (m/z): [M + Na]$^+$, calcd for C$_{31}$H$_{43}$N$_3$O$_8$S$_2$Na, 672.2384; found, 672.2393. Compound **5b**: ^{1}H NMR (500 MHz, 10% CDCl$_3$ in CD$_3$OD) δ 1.5−1.86 (m, 4H), 2.06−2.25 (m, 2H), 2.14 (dd, J = 5.2, 1.4 Hz, 1H), 2.52 (dd, J = 6.4, 1.4 Hz, 1H), 3.00 (t, J = 7.6 Hz, 2H), 3.05 (m, 1H), 3.45 (dd, J = 14.4, 6.8 Hz, 1H), 3.53 (dd, J = 14.6, 6.6 Hz, 1H), 4.39 (t, J = 6.5 Hz, 1H), 7.18 (d, J = 8.8 Hz, 2H), 7.22 (d, J = 9.2 Hz, 2H), 7.32 (d, J = 9.0 Hz, 2H), 7.93 (d, J = 9.0 Hz, 2H). HRMS-ESI (m/z): [M + H]$^+$, calcd for C$_{21}$H$_{28}$N$_3$O$_4$S$_2$, 450.1516; found, 450.1485.

Spectral Data of Glu Amide Prodrug Compound **12c**. ^{1}H NMR (500 MHz, CDCl$_3$) δ 1.47 (s, 9H), 1.49 (s, 9H), 2.00 (m, 1H), 2.17 (dd, J = 5.2, 1.8 Hz, 1H), 2.41 (m, 1H), 2.56 (m, 2H), 3.07 (m, 1H), 3.18 (dd, J = 14.3, 7.9 Hz, 1H), 3.54 (dd, J = 14.1, 5.5 Hz, 1H), 4.27 (m, 1H), 7.07 (d, J = 8.6 Hz, 2H), 7.08 (d, J = 9.0 Hz, 2H), 7.61 (d, J = 9.0 Hz, 1H), 7.86 (d, J = 9.0 Hz, 1H); ^{13}C NMR (126 MHz, CDCl$_3$) δ 24.5, 26.3, 28.2, 28.5, 37.1, 51.5, 62.8, 82.3, 117.6, 121.3, 121.9, 130.9, 131.9, 135.2, 151.0, 163.3, 169.3, 171.7. HRMS-ESI (m/z): [M + Na]$^+$, calcd for C$_{29}$H$_{38}$N$_2$O$_8$S$_2$Na, 629.1962; found, 629.1969. Compound **5c**: ^{1}H NMR (500 MHz, 10% CDCl$_3$ in CD$_3$OD) δ 2.32 (m, 1H), 2.42 (m, 1H), 2.51 (dd, J = 6.2, 1.4 Hz, 1H), 2.68 (dt, J = 7.2, 6.8, 2.0 Hz, 2H), 3.04 (m, 1H), 3.44 (dd, J = 14.4, 7.0 Hz, 1H), 3.53 (dd, J = 14.4, 6.4 Hz, 1H), 4.43 (t, J = 6.8 Hz, 1H), 4.87 (s, 10H), 7.19 (d, J = 9.2 Hz, 2H), 7.22 (d, J = 9.2 Hz, 2H), 7.32 (d, J = 9.2 Hz, 2H). HRMS-ESI (m/z): [M + H]$^+$, calcd for C$_{20}$H$_{23}$N$_2$O$_6$S$_2$, 451.0992; found, 451.1004.

Spectral Data of Arg Amide Prodrug Compound **12d**. ^{1}H NMR (500 MHz, CDCl$_3$) δ 1.38 (s, 9H), 1.48 (s, 9H), 1.53 (s, 9H), 1.59−1.96 (m, 4H), 2.16 (dd, J = 5.2, 1.8 Hz, 1H), 2.54 (dd, J = 6.2, 1.6 Hz, 1H), 3.06 (m, 1H), 3.17 (dd, J = 14.2, 8.0 Hz, 1H), 3.53 (dd, J = 14.2, 5.6 Hz, 1H), 3.72 (m, 1H), 4.12 (s, 1H), 4.55 (m, 1H), 5.99 (d, J = 8.2 Hz, 1H), 7.05 (d, J = 9.0 Hz, 2H), 7.07 (d, J = 8.8 Hz, 2H), 7.53 (d, J = 8.6 Hz, 2H), 7.85 (d, J = 9.0 Hz, 2H), 9.13 (br. s, 1H); ^{13}C NMR (126 MHz, CDCl$_3$) δ 24.5, 24.7, 26.3, 28.2, 28.6, 29.3, 44.1, 54.0, 62.8, 84.6, 117.6, 121.2, 123.4, 130.9, 132.0, 135.1, 151.3, 155.0, 161.3, 163.2, 163.4, 171.1. HRMS-ESI (m/z): [M + H]$^+$, calcd for C$_{36}$H$_{52}$N$_5$O$_{10}$S$_2$, 778.3150; found, 778.3154. Compound **5d**: ^{1}H NMR (500 MHz, 10% CDCl$_3$ in

CD$_3$OD) δ 1.71−2.11 (m, 4H), 2.16 (d, J = 5.2 Hz, 1H), 2.54 (dd, J = 6.2, 1.2 Hz, 1H), 3.06 (quin, J = 6.2 Hz, 1H), 3.29 (m, 1H), 3.45 (m, 2H), 3.54 (dd, J = 14.6, 6.4 Hz, 1H), 4.14 (m, 1H), 7.15 (d, J = 9.0 Hz, 2H), 7.15 (d, J = 9.0 Hz, 2H), 7.77 (d, J = 9.0 Hz, 2H), 7.92 (d, J = 8.8 Hz, 2H). HRMS-ESI (m/z): [M + H]$^+$, calcd for C$_{21}$H$_{28}$N$_5$O$_4$S$_2$, 478.1577; found, 478.1580.

Spectral Data of Arg-Arg Amide Prodrug Compound 12e. ^{1}H NMR (500 MHz, CDCl$_3$) δ 1.40−1.54 (5 × s, 45H), 1.46−1.90 (m, 8H), 2.16 (dd, J = 5.2, 1.8 Hz, 1H), 2.53 (dd, J = 6.2, 1.4 Hz, 1H), 3.05 (m, 1H), 3.16 (dd, J = 14.2, 7.8 Hz, 1H), 3.39 (m, 1H), 3.53 (dd, J = 14.2, 5.6 Hz, 1H), 3.55 (m, 2H), 3.82 (t, J = 6.8 Hz, 2H), 4.28 (dd, J = 13.8, 6.4 Hz, 1H), 4.59 (q, J = 7.4 Hz, 1H), 6.10 (d, J = 7.4 Hz, 1H), 7.03 (d, J = 9.0 Hz, 2H), 7.05 (d, J = 8.8 Hz, 2H), 7.22 (d, J = 6.4 Hz, 1H), 7.61 (d, J = 8.4 Hz, 2H), 7.84 (d, J = 9.0 Hz, 2H), 8.41 (t, J = 5.6 Hz, 1H), 8.84 (s, 1H), 9.26 (br. s, 1H), 9.35 (br. s, 1H), 11.47 (s, 1H); ^{13}C NMR (126 MHz, CDCl$_3$) δ 22.8, 24.5, 25.4, 26.1, 26.2, 28.2, 28.2, 28.4, 28.4, 28.6, 29.2, 31.8, 34.8, 40.1, 44.1, 53.8, 55.0, 62.8, 79.6, 80.6, 83.4, 84.3, 117.5, 121.2, 122.5, 130.9, 131.8, 135.4, 150.9, 153.4, 154.9, 156.6, 160.8, 163.4, 163.4, 163.5, 169.6. HRMS-ESI (m/z): [M + H]$^+$, calcd for C$_{52}$H$_{80}$N$_9$O$_{15}$S$_2$, 1134.5210; found, 1134.5215. Compound 5e: ^{1}H NMR (500 MHz, 10% CDCl$_3$ in CD$_3$OD) δ 1.68−2.05 (m, 8H), 2.13 (dd, J = 5.1, 1.3 Hz, 1H), 2.51 (dd, J = 6.2, 1.0 Hz, 1H), 3.17 (m, 1H), 3.22−3.28 (m, 4H), 3.42 (dd, J = 14.6, 7.0 Hz, 1H), 3.50 (dd, J = 14.0, 7.0 Hz, 1H), 4.10 (t, J = 6.3 Hz, 1H), 4.52 (dd, J = 8.7, 5.1 Hz, 1H), 7.10 (t, J = 8.9 Hz, 4H), 7.66 (d, J = 9.0 Hz, 2H), 7.89 (d, J = 9.0 Hz, 2H). HRMS-ESI (m/z): [M + H]$^+$, calcd for C$_{27}$H$_{40}$N$_9$O$_5$S$_2$, 634.2588; found, 634.2585.

4-Fluoro-2-(methoxymethoxy)-1-nitrobenzene (15). 5-Fluoro-2-nitrophenol (10 g, 63 mmol, 99%) was dissolved in anhydrous DMF (100 mL) in an oven-dried flask. The solution was stirred under an atmosphere of nitrogen and cooled in an ice−water bath. Sodium hydride (3.0 g, 75 mmol) was added with stirring, after which chloromethyl methyl ether (5.3 g, 66 mmol) was added dropwise. The resulting mixture was aged at room temperature for 1 h. The reaction was quenched with MeOH, diluted with ether, and washed with water and brine. The ether layer was dried over anhydrous Na$_2$SO$_4$ and concentrated in vacuo. Purification of the product by silica gel chromatography (hexanes/EtOAc = 1/7) gave the title compound in 88% yield. ^{1}H NMR (500 MHz, CDCl$_3$) δ 3.53 (s, 3H), 5.30 (d, J = 2.0 Hz, 2H), 6.78 (dd, J = 7.3, 9.1 Hz, 1H), 7.06 (dt, J = 2.3, 10.4 Hz, 1H), 7.91 (dd, J = 6.0, 9.0 Hz, 1 H); ^{13}C NMR (126 MHz, CDCl$_3$) δ 57.0, 95.6, 105.0 (d, J = 26.3 Hz), 108.8 (d, J = 23.0 Hz), 127.8 (d, J = 10.7 Hz), 152.8 (d, J = 11.5 Hz), 165.5 (d, J = 255.9 Hz). HRMS-FAB (m/z): [M + Na]$^+$, calcd for C$_8$H$_8$FNNaO$_4$, 224.0330; found, 224.0328.

S-(4-(3-(Methoxymethoxy)-4-nitrophenoxy)phenyl) Dimethylcarbamothioate (17). To a round-bottom flask was added dimethylcarbamothioate 16 (2.1 g, 11 mmol), compound 15 (2.5 g, 12 mmol), DMF (50 mL), and Cs$_2$CO$_3$ (7.1 g, 22 mmol). The resulting mixture was stirred for 24 h, followed by filtration through a layer of silica gel. The solvent was evaporated, and the product was purified by silica gel chromatography (hexanes/EtOAc = 2/1) to give 17 as a solid in 88% (3.5 g). ^{1}H NMR (500 MHz, CDCl$_3$) δ 3.05 (br. s., 3H), 3.12 (br. s., 3H), 3.53 (s, 3H), 5.28 (s, 2H), 6.61 (ddd, J = 0.8, 2.5, 9.1 Hz, 1H), 6.99 (d, J = 2.4 Hz, 1H), 7.02−7.12 (m, 2H), 7.50−7.56 (m, 2H), 7.88−7.93 (m, 1 H); ^{13}C NMR (126 MHz, CDCl$_3$) δ 37.1, 37.2, 57.1, 95.5, 107.1, 110.4, 120.5, 125.1, 127.9, 135.7, 137.9, 153.0, 156.1, 162.0, 166.9. HRMS-FAB (m/z): [M + H]$^+$, calcd for C$_{17}$H$_{19}$N$_2$O$_6$S, 379.0958; found, 379.0945.

t-Butyl (4-(4-((Dimethylcarbamoyl)thio)phenoxy)-2-(methoxymethoxy)phenyl)carbamate (18). A solution of 17 (2.5 g, 6.6 mmol) in MeOH/H$_2$O (30 mL/15 mL) was treated with elemental iron (1.9 g, 34 mmol) and NH$_4$Cl (0.35 g, 6.5 mmol), and the resulting mixture was heated at reflux for 2 h. The crude reaction mixture was filtered through Celite, and the filtrate was concentrated in vacuo. The residue was dissolved in EtOAc and was washed with water. The organic layer was separated, and the aqueous layer was washed with EtOAc. The combined organic portions were dried over anhydrous Na$_2$SO$_4$. The solvent was removed under reduced pressure to provide the amine as a solid (1.9 g, 5.5 mmol, 83%). This product was dissolved in MeOH (30 mL), treated with TEA (0.6 g, 5.9 mmol) and Boc$_2$O (1.9 g, 8.4 mmol, 97%), and stirred at room temperature for 24 h. The solvent was removed under reduced pressure, and the product was purified by silica gel chromatography (hexanes/EtOAc = 3/1) to give the title compound (1.9 g, 76%). ^{1}H NMR (500 MHz, CDCl$_3$) δ 1.54 (s, 9H), 3.02 (br. s., 3H), 3.08 (br. s., 3H), 3.48 (s, 3H), 5.18 (s, 2H), 6.71 (dd, J = 2.6, 8.8 Hz, 1H), 6.90 (d, J = 2.6 Hz, 1H), 6.92−6.97 (m, 2H), 7.00 (br. s., 1H), 7.36−7.42 (m, 2H), 8.05 (br. s., 1 H); ^{13}C NMR (126 MHz, CDCl$_3$) δ 28.4, 36.9, 56.5, 80.5, 95.3, 107.2, 113.6, 117.7, 119.3, 121.6, 125.3, 137.4, 146.5, 150.6, 152.9, 159.4, 167.4. HRMS-FAB (m/z): [M + H]$^+$, calcd for C$_{22}$H$_{29}$N$_2$O$_6$S, 449.1741; found, 449.1735.

t-Butyl (2-(Methoxymethoxy)-4-(4-((oxiran-2-ylmethyl)thio)phenoxy)phenyl)carbamate (19). To a solution of compound 18 (0.65 g, 1.5 mmol) in anhydrous MeOH (10 mL) was added potassium hydroxide (0.42 g, 7.5 mmol). The mixture was refluxed for 4 h and then cooled to room temperature. Epichlorohydrin (0.21 g, 2.3 mmol) was added dropwise, and the mixture was stirred at room temperature for 15 min, after which the solvent was removed under reduced pressure. The concentrate was diluted with water and extracted with EtOAc. The combined organic extracts were dried over anhydrous Na$_2$SO$_4$, and the suspension was filtered, followed by concentration of the filtrate in vacuo. Purification by silica gel chromatography (hexanes/EtOAc = 4/1) gave 19 in 68% yield (0.43 g). ^{1}H NMR (500 MHz, CDCl$_3$) δ 1.53 (s, 9H), 2.47 (dd, J = 2.6, 5.0 Hz, 1H), 2.77 (t, J = 4.4 Hz, 1H), 2.85 (dd, J = 6.1, 13.9 Hz, 1H), 3.05−3.12 (m, 1H), 3.12−3.18 (m, 1H), 5.18 (s, 2H), 3.48 (s, 3H), 6.66 (dd, J = 2.6, 8.8 Hz, 1H), 6.85−6.92 (m, 3H), 6.98 (br. s., 1H), 7.37−7.44 (m, 2 H), 8.03 (br. s., 1H); ^{13}C NMR (126 MHz, CDCl$_3$) δ 28.5, 38.2, 47.6, 51.3, 56.5, 80.6, 95.4, 106.8, 113.1, 118.4, 119.4, 125.1, 128.0, 131.8, 133.8, 146.6, 151.2, 152.9, 157.9. HRMS-FAB (m/z): [M + H]$^+$, calcd for C$_{22}$H$_{28}$NO$_4$S, 434.1632; found, 434.1637.

t-Butyl (2-(Methoxymethoxy)-4-(4-((oxiran-2-ylmethyl)sulfonyl)phenoxy)phenyl)carbamate (20). Compound 19 (0.44 g, 1.0 mmol) was dissolved in CH$_2$Cl$_2$ (10 mL) and cooled in an ice−water bath. It was treated with m-CPBA (0.48 g, 2.1 mmol, 77%), and the resulting white suspension was stirred at room temperature for 10 min. The mixture was filtered, and the filtrate was washed with saturated Na$_2$S$_2$O$_3$, followed by saturated NaHCO$_3$. The organic layer was separated, and the aqueous layer was washed with CH$_2$Cl$_2$. The combined organic solution was dried over anhydrous Na$_2$SO$_4$, the suspension was filtered, and the filtrate was concentrated in vacuo. Purification of the product by silica gel chromatography (hexanes/EtOAc = 2/1) gave the title compound in 89% yield (0.42 g). ^{1}H NMR (500 MHz, CDCl$_3$) δ 1.54 (s, 9H), 2.48 (dd, J = 2.2, 4.8 Hz, 1H), 2.82 (t, J = 4.5 Hz, 1H), 3.19−3.28 (m, 1H), 3.28−3.38 (m, 2H), 3.49 (s, 3H), 5.20 (s, 2H), 6.73 (dd, J = 2.6, 8.8 Hz, 1H), 6.91 (d, J = 2.6 Hz, 1H), 7.03 (s, 1H), 7.04−7.09 (m, 2H), 7.83−7.89 (m, 2H), 8.13 (br. s., 1 H); ^{13}C NMR (126 MHz, CDCl$_3$) δ 28.5, 46.0, 46.1, 56.6, 59.8, 80.9, 95.4, 107.5, 114.2, 117.2, 119.5, 126.3, 130.6, 132.3, 146.7, 149.4, 152.9, 163.5. HRMS-FAB (m/z): [M + H]$^+$, calcd for C$_{22}$H$_{28}$NO$_8$S, 466.1530; found, 466.1543.

t-Butyl (2-(Methoxymethoxy)-4-(4-((thiiran-2-ylmethyl)sulfonyl)phenoxy)phenyl)carbamate (21). To a solution of 20 (0.40 g, 0.86 mmol) in CH$_2$Cl$_2$ (5 mL) was added a mixture of thiourea (0.10 g, 1.3 mmol, 99%) in methanol (5 mL). The resulting mixture was stirred for 24 h at room temperature, after which the solvent was removed under reduced pressure. The residue was partitioned between CH$_2$Cl$_2$ and water. The organic layer was dried over anhydrous Na$_2$SO$_4$ and was filtered. Evaporation of solvent and purification by silica gel chromatography (hexanes/EtOAc = 4/1) gave 0.34 g of 21 (83%). ^{1}H NMR (500 MHz, CDCl$_3$) δ 1.53 (s, 9H), 2.14 (dd, J = 1.8, 5.0 Hz, 1H), 2.52 (dd, J = 1.5, 5.9 Hz, 1H), 3.04 (dq, J = 5.6, 7.8 Hz, 1H), 3.15 (dd, J = 8.0, 14.2 Hz, 1H), 3.47 (s, 3H), 3.51 (dd, J = 5.6, 14.4 Hz, 1H), 5.19

(s, 2H), 6.72 (dd, J = 2.6, 8.8 Hz, 1H), 6.91 (d, J = 2.6 Hz, 1H), 7.01–7.08 (m, 3H), 7.80–7.85 (m, 2H), 8.08–8.16 (m, 1 H); ^{13}C NMR (126 MHz, CDCl$_3$) δ 24.4, 26.2, 28.5, 56.6, 62.7, 80.8, 95.3, 107.3, 114.1, 117.3, 119.4, 126.2, 130.8, 131.6, 146.6, 149.3, 152.8, 163.5. HRMS-FAB (m/z): [M + H]$^+$, calcd for C$_{22}$H$_{28}$NO$_7$S$_2$, 482.1302; found, 482.1301.

2-Amino-5-(4-((thiiran-2-ylmethyl)sulfonyl)phenoxy)phenol (13). To a solution of compound **21** (0.10 g, 0.21 mmol) in methanol (5 mL) was added a few drops of concd HCl. After the mixture was stirred at reflux for 1 h, the solvent was evaporated in vacuo. The crude product was taken up into water and EtOAc. Layers were separated, and the aqueous layer was washed with EtOAc. The combined organic layers were dried over anhydrous Na$_2$SO$_4$, the suspension was filtered, and the filtrate was concentrated in vacuo. Purification by silica gel chromatography (hexanes/EtOAc = 1/1) gave **13** in 95% yield (66 mg). ^{1}H NMR (500 MHz, CDCl$_3$) δ 2.14 (dd, J = 1.3, 4.9 Hz, 1H), 2.18 (d, J = 1.0 Hz, 1H), 2.49–2.56 (m, 1H), 3.00–3.08 (m, 1H), 3.17 (dd, J = 7.8, 14.4 Hz, 1H), 3.51 (dd, J = 5.6, 14.2 Hz, 2H), 6.46–6.54 (m, 2H), 6.73–6.80 (m, 1H), 6.97–7.07 (m, 2H), 7.80 (m, 2 H); ^{13}C NMR (126 MHz, CDCl$_3$) δ 24.4, 26.3, 62.8, 108.5, 113.1, 117.2, 117.9, 130.7, 131.1, 131.9, 145.9, 147.3, 164.1. HRMS-FAB (m/z): [M + H]$^+$, calcd for C$_{15}$H$_{16}$NO$_4$S$_2$, 338.0515; found, 338.0507.

N-(4-(4-((Thiiran-2-ylmethyl)sulfonyl)phenoxy)phenyl) hydroxylamine (14). Compound **22** (75 mg, 0.21 mmol), prepared as described previously,[28] in CH$_2$Cl$_2$/H$_2$O (0.2 mL/0.1 mL) was treated with Zn (50 mg, 0.76 mmol) and NH$_4$Cl (25 mg, 0.47 mmol). The resulting mixture was stirred for 30 min at room temperature. It was then filtered over Celite, and the filtrate was concentrated in vacuo. Purification by silica gel chromatography (CH$_2$Cl$_2$) gave **14** in 69% yield (50 mg). ^{1}H NMR (500 MHz, CDCl$_3$) δ 2.16 (dd, J = 1.8, 5.2 Hz, 1H), 2.53 (dd, J = 1.0, 6.2 Hz, 1H), 3.01–3.09 (m, 1H), 3.17 (dd, J = 7.9, 14.3 Hz, 1H), 3.53 (dd, J = 5.8, 14.2 Hz,1H), 6.98–7.10 (m, 6H), 7.81–7.88 (m, 2 H); ^{13}C NMR (126 MHz, CDCl$_3$) δ 24.5, 26.3, 62.8, 116.5, 117.3, 121.6, 130.9, 131.5, 147.4, 149.4, 163.8. HRMS-FAB (m/z): [M + H]$^+$, calcd for C$_{15}$H$_{16}$NO$_4$S$_2$, 338.0515; found, 338.0501.

Solubility Determination and Solution Stability. The water solubilities of the prodrugs were measured at room temperature by using a 10 mg/mL solution of each compound in water. The molar extinction coefficient was calculated at 245 nm. The aqueous solutions were centrifuged, and the absorbance at 245 nm of the supernatant was recorded. The concentration was calculated using Beer's law. Assays were performed in triplicate. The ester and amide prodrugs had solubilities of over 10 mg/mL. Over a period of one month, appropriately diluted aliquots were analyzed by HPLC for the presence of the prodrug and the active gelatinase inhibitors (compound **2** from the esters or compound **3** from the amides).

Ex Vivo Hydrolyses of the Amide Prodrugs. Fresh blood was collected in heparinized syringes from human volunteers. Blood collection from human volunteers was approved by the University of Notre Dame Institutional Review Board. The blood was centrifuged to obtain plasma. The stability of the prodrugs in plasma and whole blood (1 mL) was determined by spiking the plasma or blood with 10 μL of 10 mM of the prodrug and incubating at 37 °C. Aliquots were drawn periodically and processed for analysis. For the plasma samples, the reaction was immediately terminated by the addition of two volumes of acetonitrile. For the blood samples, aliquots were first centrifuged at 4 °C, and the resultant plasma was treated with two volumes of acetonitrile. The precipitated protein was centrifuged (10 min, 10 500g), and the supernatant was analyzed by reversed-phase HPLC with UV detection. First-order rate constants for the disappearance of the prodrugs were calculated from which the half-lives were determined.

Enzyme Inhibition Studies. Human recombinant active MMP-2 and MMP-7 and catalytic domains of MMP-3 and MMP-14 were purchased from EMD Biosciences (La Jolla, CA, USA). The catalytic domains of human recombinant MMP-1 and MMP-9 were from Biomol International (Plymouth Meeting, PA, USA). The fluorogenic substrate

MOCAcPLGLA$_2$pr(Dnp)AR-NH$_2$ was purchased from Peptides International (Louisville, KY, USA); MOCAcRPKPVE(Nva)WRK(Dnp)-NH$_2$ and (Dnp)P(Cha)GC(Me)HAK(NMa)NH$_2$ were obtained from R&D Systems (Minneapolis, MN, USA). The K_m values used for the reaction of MMP-2, MMP-9, and MMP-14 with the fluorogenic substrate MOCAcPLGLA$_2$pr(Dnp)AR-NH$_2$ were 18.9 ± 1.0, 5.0 ± 0.1, and 5.6 ± 0.4 μM, respectively. Inhibitor stock solutions (10 mM) were prepared in water (except for compound **13**, which was prepared in DMSO). The methodology for enzyme inhibition and assays was the same as that reported previously.[28] Substrate hydrolysis was measured with a Cary Eclipse fluorescence spectrophotometer (Varian, Walnut Creek, CA, USA).

Microsomal Incubations. Mouse, rat, and human liver microsomes and rat S9 were purchased from BD Biosciences (Woburn, MA, USA). Incubations consisted of liver microsomes (1.0 mg), NADPH (0.5 mM, final concentration), and 100 μM compound (final concentration) in potassium phosphate buffer (100 mM, pH 7.4) at 37 °C in a total volume of 1 mL. Aliquots were drawn at different time points, and the reactions were terminated by the addition of one volume of acetonitrile containing 25 μM (S)-2-((S)-1-((4-phenoxyphenyl)sulfonyl)-ethyl)thiirane, prepared as published,[22] as an internal standard. The precipitated protein was centrifuged (10 min, 10 500g), and the supernatant was analyzed by reversed-phase HPLC with UV detection.

Apparent Intrinsic Clearance (CL$_{int,app}$) Determination in Microsomes. Apparent intrinsic clearance was calculated by the following equation:[39]

$$CL_{int,app} = (0.693/\text{in vitro } t_{1/2})$$
$$\times (\text{incubation volume/mg of microsomal protein})$$
$$\times (45 \text{ mg of microsomal protein/gram of liver})$$
$$\times (20 \text{ g of liver/kg body weight})$$

In the previous equation, the weight of the liver can be 20, 45, or 90 g of liver/kg of body weight for human, rat, and mouse, respectively.

High-Performance Liquid Chromatography. The HPLC system consisted of a Perkin-Elmer series 200 quaternary pump (Perkin-Elmer Corp., Norwalk, CT, USA), a Perkin-Elmer UV detector series 200, and a Perkin-Elmer autosampler series 200 with a thermostatted tray. Samples were analyzed on a YMC 5 μm basic column (4.6 mm i.d. × 150 mm, YMC Inc., Wilmington, NC, USA) connected to a YMC 5 μm basic guard cartridge (4.0 mm i.d. × 20 mm). The mobile phase consisted of elution at 1 mL/min with 75% A/25% B for 3 min, followed by a 17-min linear gradient to 10% A/90% B, then 10% A/90% B for 5 min (A = 100 mM NH$_4$OAc at pH 4; B = acetonitrile). Effluent was monitored by UV detection at 245 nm.

Liquid Chromatography–Mass Spectrometry. The LC system consisted of a Dionex Ultimate 3000 RSLC (Dionex, Sunnyvale, CA, USA) equipped with a Dionex Ultimate 3000 autosampler and a Dionex Ultimate 3000 diode array detector. All mass spectrometric experiments were performed with a Bruker MicroTOF-Q II (Billerica, MA, USA) monitored with Hystar 3.2 software. Mass spectrometry acquisition was performed using electrospray ionization with the following parameters: end plate offset voltage = −0.5 kV, capillary voltage = 4.5 kV, and nitrogen as both a nebulizer and dry gas (8.0 L/min flow rate, 200 °C dry temperature, 4.0 bar). Samples were analyzed on an Acclaim RSLC 120 C18 column (2.2 μm, 2.1 mm i.d. × 100 mm, Dionex, Sunnyvale, CA, USA). The mobile phase consisted of elution at 0.5 mL/min with 85% A/15% B for 3 min, followed by a 9-min linear gradient to 10% A/90% B, and then 10% A/90% B for 2 min (A = 0.1% formic acid in water; B = 0.1% formic acid in acetonitrile).

AMES II Mutagenecity Assay. The Ames II mutagenecity assay was carried out by BioReliance (Rockville, MD, USA). Briefly, the strains included the Ames II mixed strains (TA7001 to TA7006) and tester strain TA98, as described.[34] The strains were mixed with the test article

(**5d** or **3**) and appropriate metabolic activation mixture. The mixture was incubated at 37 °C for 90 min. The mixture was then mixed with an indicator medium, and the contents were plated in 384-well plates. After 48 h of incubation, the plates were scored for positive wells. The test article was tested at a maximum of six dose levels (3.3, 10.0, 33.3, 100.0, 333.3, and 1000 μg/mL) along with appropriate negative and positive controls with mixed Ames II strains and tester strain TA98, with and without S9 activation. All dose levels of the test article, negative controls, and positive controls were tested in triplicate. 2-Aminoanthracene (5.0 μg/mL) and 4-nitroquinoline N-oxide (1.0 μg/mL) were used as positive controls with S9 activation. 2-Nitrofluorene (2.0 μg/mL) was used as a positive control without S9 activation.

Animals. Male C57Bl/6J mice (The Jackson Laboratory, Bar Harbor, ME, USA), 6−8 weeks old, 22−25 g body weight, specific pathogen free, were provided with Laboratory 5001 Rodent Diet (PMI, Richmond, IN, USA) and water ad libitum. Animals were maintained in polycarbonate shoebox cages with hardwood bedding in a room under a 12:12 h light/dark cycle and at 72 ± 2 °F. Animal studies were approved by the University of Notre Dame Institutional Animal Care and Use Committee.

Animal Dosing and Sample Collection. Compounds **5d** and **3**, as HCl salts, were dissolved in saline to a final concentration of 2.5 mg/mL. The solution was sterilized by passage through an Acrodisc syringe filter (Pall Life Sciences, 0.2 μm, 13 mm diameter, PTFE membrane). Mice ($n = 3$ per time point per compound) received a single 120 μL dose of **5d** or **3** intravenously (equivalent to 12.5 mg/kg) by tail vein injection. Mice used for later time points (1 h, 2 h, and 4 h) were housed in Nalgene rat metabolic cages equipped with flooring grates and feeders for mice (Tecniplast, West Chester, PA, USA), for easy collection of urine. Terminal blood samples were collected at various time points by cardiac puncture following CO_2 asphixation, using heparin as an anticoagulant. Blood was stored on ice and centrifuged to obtain plasma. Urine samples were collected, pooled by time point (1 h, 2 h, and 4 h), and stored on ice.

Sample Analysis. A 200-μL aliquot of plasma was mixed with 400 μL of 1 μM (S)-2-((S)-1-((4-phenoxyphenyl)sulfonyl)ethyl)thiirane as the internal standard in acetonitrile. The sample was centrifuged at 10 000g for 20 min. The supernatant was concentrated, reconstituted to 120 μL with water, and analyzed by reversed-phase LC with MS detection at m/z 478.1577 (for **5d**), m/z 322.0566 (for **3**), and m/z 364.0672 (for the p-N-acetyl derivative, M3). Standard curves of **5d**, **3**, and the p-N-acetyl derivative in blank mouse plasma were prepared by fortification of 200 μL of plasma with each compound at concentrations of 0, 0.005, 0.01, 0.025, 0.05, 0.1, 0.25, 0.5, 1, 2.5, 5, 10, 25, and 50 μM. Quantification of **5d**, **3**, and the p-N-acetyl derivative (M3) was performed using peak area ratios relative to the internal standard and linear regression parameters calculated from the calibration curve standards prepared in blank mouse plasma. The assay was linear from 0.005 to 50 μM, with coefficients of determination, R^2, of 0.998 for **5d**, 0.999 for **3**, and 0.999 for the p-N-acetyl derivative.

Urine samples were centrifuged at 10 000g for 10 min, and a 50-μL aliquot of each supernatant was analyzed by LC/MS. In addition to analyzing for **5d**, **3**, and p-N-acetyl M3, the plasma and urine samples were screened specifically for N-hydroxylamine **14** with MS detection at m/z 338.0515.

Pharmacokinetic Parameters. Pharmacokinetic parameters were determined by noncompartmental analyses of the concentration−time data for **5** and **3**. Area under the concentration−time curve (AUC) was determined by the linear trapezoidal rule. The concentration at time = 0 (C_0) was estimated from the first sampling times by back-extrapolation using log−linear regression analysis. $AUC_{0-\infty}$ was calculated as $AUC_{0-t} + (C_{last}/k)$, where AUC_{0-t} is the area under the mean plasma concentration−time curve up to the last quantifiable sample, and C_{last} is the concentration at the last quantifiable sampling time. Half-lives ($t_{1/2}$) were estimated from the terminal linear portion of the concentration−time data by linear regression, where the slope of the line was the rate constant k, and $t_{1/2} = \ln 2/k$. Volume of distribution (Vd) was calculated as the dose divided by the initial concentration (C_0). Clearance (CL) was calculated from the dose divided by $AUC_{0-\infty}$. Concentrations of **3** and the p-N-acetyl derivative (M3) after intravenous administration of **3** at 12.5 mg/kg were normalized to 8.13 mg/kg (equivalent to 12.5 mg/kg intravenous administration of **5d**).

■ AUTHOR INFORMATION

Corresponding Author
*Tel: +1-574-631-2965. Fax: +1-574-631-6652. E-mail: mchang@nd.edu.

Author Contributions
§These authors contributed equally to this work.

■ ABBREVIATIONS USED

amu, atomic mass unit; AUC, area under the concentration−time curve; Boc, tert-butoxycarbonyl; CL, clearance; DMAP, 4-(dimethylamino)pyridine; DMSO, dimethyl sulfoxide; Dnp, 2,4-dinitrophenyl; HPLC, high-performance liquid chromatography; M1(−5), metabolite 1(−5); m-CBPA, meta-chloroperbenzoic acid; MMP, matrix metalloproteinase; MOCAc, (7-methoxy-coumarin-4-yl)acetyl; MOM, methoxymethyl; MS, mass spectrometry; NADPH, nicotinamide adenine dinucleotide phosphate reduced; NHS, N-hydroxysuccinimide; Nva, L-norvalyl; Vd, volume of distribution

■ REFERENCES

(1) Moses, M. A. The regulation of neovascularization by matrix metalloproteinases and their inhibitors. *Stem Cells* **1997**, *15*, 180–189.

(2) Nguyen, M.; Arkell, J.; Jackson, C. J. Human endothelial gelatinases and angiogenesis. *Int. J. Biochem. Cell Biol.* **2001**, *33*, 960–970.

(3) Stamenkovic, I. Extracellular matrix remodelling: the role of matrix metalloproteinases. *J. Pathol.* **2003**, *200*, 448–464.

(4) Sorokin, L. The impact of the extracellular matrix on inflammation. *Nat. Rev. Immunol.* **10**, 712-23.

(5) Agrawal, S.; Anderson, P.; Durbeej, M.; van Rooijen, N.; Ivars, F.; Opdenakker, G.; Sorokin, L. M. Dystroglycan is selectively cleaved at the parenchymal basement membrane at sites of leukocyte extravasation in experimental autoimmune encephalomyelitis. *J. Exp. Med.* **2006**, *203*, 1007–19.

(6) Kessenbrock, K.; Plaks, V.; Werb, Z. Matrix metalloproteinases: regulators of the tumor microenvironment. *Cell* **2010**, *141*, 52–67.

(7) Massova, I.; Kotra, L. P.; Fridman, R.; Mobashery, S. Matrix metalloproteinases: structures, evolution, and diversification. *FASEB J.* **1998**, *12*, 1075–1095.

(8) Montaner, J.; Alvarez-Sabin, J.; Molina, C. A.; Angles, A.; Abilleira, S.; Arenillas, J.; Monasterio, J. Matrix metalloproteinase expression is related to hemorrhagic transformation after cardioembolic stroke. *Stroke* **2001**, *32*, 2762–2767.

(9) Fisher, J. F.; Mobashery, S. Recent advances in MMP inhibitor design. *Cancer Metastasis Rev.* **2006**, *25*, 115–136.

(10) Hu, J.; Van den Steen, P. E.; Sang, Q. X.; Opdenakker, G. Matrix metalloproteinase inhibitors as therapy for inflammatory and vascular diseases. *Nat. Rev. Drug Discovery* **2007**, *6*, 480–98.

(11) Brown, S.; Bernardo, M. M.; Li, Z. H.; Kotra, L. P.; Tanaka, Y.; Fridman, R.; Mobashery, S. Potent and selective mechanism-based inhibition of gelatinases. *J. Am. Chem. Soc.* **2000**, *122*, 6799–6800.

(12) Forbes, C.; Shi, Q. C.; Fisher, J. F.; Lee, M.; Hesek, D.; Llarrull, L. I.; Toth, M.; Gossing, M.; Fridman, R.; Mobashery, S. Active site ring-opening of a thiirane moiety and picomolar inhibition of gelatinases. *Chem. Biol. Drug Des.* **2009**, *74*, 527–534.

(13) Bonfil, R. D.; Sabbota, A.; Nabha, S.; Bernardo, M. M.; Dong, Z.; Meng, H.; Yamamoto, H.; Chinni, S. R.; Lim, I. T.; Chang, M.; Filetti, L. C.; Mobashery, S.; Cher, M. L.; Fridman, R. Inhibition of human prostate cancer growth, osteolysis and angiogenesis in a bone metastasis model by a novel mechanism-based selective gelatinase inhibitor. *Int. J. Cancer* **2006**, *118*, 2721–2726.

(14) Martin, M. D.; Carter, K. J.; Jean-Philippe, S. R.; Chang, M.; Mobashery, S.; Thiolloy, S.; Lynch, C. C.; Matrisian, L. M.; Fingleton, B. Effect of ablation or inhibition of stromal matrix metalloproteinase-9 on lung metastasis in a breast cancer model is dependent on genetic background. *Cancer Res.* **2008**, *68*, 6251–6259.

(15) Kruger, A.; Arlt, M. J. E.; Gerg, M.; Kopitz, C.; Bernardo, M. M.; Chang, M.; Mobashery, S.; Fridman, R. Antimetastatic activity of a novel mechanism-based gelatinase inhibitor. *Cancer Res.* **2005**, *65*, 3523–3526.

(16) Gu, Z. Z.; Cui, J.; Brown, S.; Fridman, R.; Mobashery, S.; Strongin, A. Y.; Lipton, S. A. A highly specific inhibitor of matrix metalloproteinase-9 rescues laminin from proteolysis and neurons from apoptosis in transient focal cerebral ischemia. *J. Neurosci.* **2005**, *25*, 6401–6408.

(17) Guo, Z. D.; Sun, X. C.; He, Z. H.; Jiang, Y.; Zhang, X. D.; Zhang, J. H. Matrix metalloproteinase-9 potentiates early brain injury after subarachnoid hemorrhage. *Neurol. Res.* **2010**, *32*, 715–720.

(18) Ota, R.; Kurihara, C.; Tsou, T. L.; Young, W. L.; Yeghiazarians, Y.; Chang, M.; Mobashery, S.; Sakamoto, A.; Hashimoto, T. Roles of matrix metalloproteinases in flow-induced outward vascular remodeling. *J. Cereb. Blood Flow Metab.* **2009**, *29*, 1547–1558.

(19) Yu, F.; Kamada, H.; Niizuma, K.; Endo, H.; Chan, P. H. Induction of MMP-9 expression and endothelial injury by oxidative stress after spinal cord injury. *J. Neurotrauma* **2008**, *25*, 184–195.

(20) Testero, S. A.; Lee, M.; Staran, R. T.; Espahbodi, M.; Llarrull, L. I.; Toth, M.; Mobashery, S.; Chang, M. Sulfonate-containing thiiranes as selective gelatinase inhibitors. *ACS Med. Chem. Lett.* **2011**, *2*, 177–181.

(21) Lee, M.; Villegas-Estrada, A.; Celenza, G.; Boggess, B.; Toth, M.; Kreitinger, G.; Forbes, C.; Fridman, R.; Mobashery, S.; Chang, M. Metabolism of a highly selective gelatinase inhibitor generates active metabolite. *Chem. Biol. Drug Des.* **2007**, *70*, 371–382.

(22) Gooyit, M.; Lee, M.; Hesek, D.; Boggess, B.; Oliver, A. G.; Fridman, R.; Mobashery, S.; Chang, M. Synthesis, kinetic characterization and metabolism of diastereomeric 2-(1-(4-phenoxyphenylsulfonyl)ethyl)thiiranes as potent gelatinase and MT1-MMP inhibitors. *Chem. Biol. Drug Des.* **2009**, *74*, 535–546.

(23) Lee, M.; Celenza, G.; Boggess, B.; Blase, J.; Shi, Q.; Toth, M.; Bernardo, M. M.; Wolter, W. R.; Suckow, M. A.; Hesek, D.; Noll, B. C.; Fridman, R.; Mobashery, S.; Chang, M. A potent gelatinase inhibitor with anti-tumor-invasive activity and its metabolic disposition. *Chem. Biol. Drug Des.* **2009**, *73*, 189–202.

(24) Stella, V. J. Prodrug strategies for improving drug-like properties. In *Optimizing the "Drug-Like" Properties of Leads in Drug Discovery*, Borchardt, R. T., Kerns, E. H., Hageman, M. J., Thakker, D. R., Stevens, J. L., Eds.; Springer Science and Business Media: New York, 2006; Vol. IV, pp 221–237.

(25) Stella, V. J.; Nti-Addae, K. W. Prodrug strategies to overcome poor water solubility. *Adv. Drug Delivery Rev.* **2007**, *59*, 677–694.

(26) Nam, N. H.; Kim, Y.; You, Y. J.; Hong, D. H.; Kim, H. M.; Ahn, B. Z. Water soluble prodrugs of the antitumor agent 3-[3-amino-4-methoxy)phenyl]-2-(3,4,5-trimethoxyphenyl)cyclopent-2-ene-1-one. *Bioorg. Med. Chem.* **2003**, *11*, 1021–1029.

(27) Pochopin, N. L.; Charman, W. N.; Stella, V. J. Amino-acid derivatives of dapsone as water-soluble prodrugs. *Int. J. Pharm.* **1995**, *121*, 157–167.

(28) Ikejiri, M.; Bernardo, M. M.; Bonfil, R. D.; Toth, M.; Chang, M. L.; Fridman, R.; Mobashery, S. Potent mechanism-based inhibitors for matrix metalloproteinases. *J. Biol. Chem.* **2005**, *280*, 33992–34002.

(29) Lee, M.; Bernardo, M. M.; Meroueh, S. O.; Brown, S.; Fridman, R.; Mobashery, S. Synthesis of chiral 2-(4-phenoxyphenylsulfonyl-methyl)thiiranes as selective gelatinase inhibitors. *Org. Lett.* **2005**, *7*, 4463–4465.

(30) Lim, I. T.; Brown, S.; Mobashery, S. A convenient synthesis of a selective gelatinase inhibitor as an antimetastatic agent. *J. Org. Chem.* **2004**, *69*, 3572–3573.

(31) Davies, B.; Morris, T. Physiological-parameters in laboratory-animals and humans. *Pharm. Res.* **1993**, *10*, 1093–1095.

(32) Tanaka, K.; Yamamoto, Y.; Kuzuya, A.; Komiyama, M. Synthesis of photo-responsive acridine-modified DNA and its application to site-selective RNA scission. *Nucleosides, Nucleotides Nucleic Acids* **2008**, *27*, 1175–1185.

(33) Coleman, M. D. *Human Drug Metabolism*; John Wiley & Sons, Ltd.: New York, 2005.

(34) Gee, P.; Maron, D. M.; Ames, B. N. Detection and classification of mutagens: a set of base-specific salmonella tester strains. *Proc. Natl. Acad. Sci. U.S.A.* **1994**, *91*, 11606–11610.

(35) Sato, H.; Takino, T.; Okada, Y.; Cao, J.; Shinagawa, A.; Yamamoto, E.; Seiki, M. A matrix metalloproteinase expressed on the surface of invasive tumor-cells. *Nature* **1994**, *370*, 61–65.

(36) Deryugina, E. I.; Ratnikov, B.; Monosov, E.; Postnova, T. I.; DiScipio, R.; Smith, J. W.; Strongin, A. Y. MT1-MMP initiates activation of pro-MMP-2 and integrin alpha v beta 3 promotes maturation of MMP-2 in breast carcinoma cells. *Exp. Cell Res.* **2001**, *263*, 209–223.

(37) Schywalsky, M.; Ihmsen, H.; Tzabazis, A.; Fechner, J.; Burak, E.; Vornov, J.; Schwilden, H. Pharmacokinetics and pharmacodynamics of the new propofol prodrug GPI 15715 in rats. *Eur. J. Anaesthesiol.* **2003**, *20*, 182–90.

(38) Fechner, J.; Schwilden, H.; Schuttler, J. Pharmacokinetics and pharmacodynamics of GPI 15715 or fospropofol (Aquavan injection): a water-soluble propofol prodrug. *Handb. Exp. Pharmacol.* **2008**, 253–66.

(39) Lu, C.; Li, P.; Gallegos, R.; Uttamsingh, V.; Xia, C. Q.; Miwa, G. T.; Balani, S. K.; Gan, L. S. Comparison of intrinsic clearance in liver microsomes and hepatocytes from rats and humans: evaluation of free fraction and uptake in hepatocytes. *Drug Metab. Dispos.* **2006**, *34*, 1600–1605.